



Contents lists available at ScienceDirect

Computer Communications

journal homepage: www.elsevier.com/locate/comcom

On improving SINR in LTE HetNets with D2D relays

Vanlin Sathya*, Arun Ramamurthy, S. Sandeep Kumar, Bheemarjuna Reddy Tamma

Department of Computer Science and Engineering, Indian Institute of Technology Hyderabad, Hyderabad, India

ARTICLE INFO

Article history:

Received 6 July 2015

Revised 13 October 2015

Accepted 19 December 2015

Available online xxx

Keywords:

Femto cells

LTE

SINR

HetNets

D2D

ABSTRACT

Femtos, with frequency reuse one, can be deployed in hotspots, offices and residences alike to provide high indoor data rates and reduce traffic load on Macro. However, arbitrarily deployed Femtos could decrease SINR significantly because of inter-cell interference and obstacles present in the building. Hence, to attain a desirable SINR Femtos have to be placed efficiently. At the same time, minimizing the power leakage from indoor Femtos in order to improve the SINR of outdoor users in the high interference zone (HIZone) around building areas is also important. To guarantee minimum SINR to both indoor UEs (*IUEs*) and outdoor UEs in HIZone (*HIZUEs*), we apply the concept of device-to-device (D2D) communication wherein free/idle *IUEs* act like UE-relays for *HIZUEs*. We first formulate a D2D MILP model which establishes D2D pairs between free/idle *IUEs* and *HIZUEs* and also guarantees certain SINR threshold ($SINR_{r,h}$) for both *IUEs* and *HIZUEs*. As D2D MILP model takes more computation time, it is not usable in real-world scenarios for establishing D2D pairs on the fly. Hence, we propose a two-step D2D heuristic algorithm for establishing D2D based relay pairs. In step one (called as hDPRA), it efficiently chooses potential D2D based relay pairs and allocates radio resources to them. In step two (called as hDPA), a Linear Programming (LP) model is formulated for power control of D2D links. We have evaluated the performance of the proposed D2D heuristic algorithm for different scenarios (i.e., 500 topologies) by varying densities of *IUEs* and *HIZUEs*. From our evaluation, we find that the proposed algorithm maintains almost the same SINR as that of *Full Power Femto scheme* (i.e., Femto transmits with maximum power) for *IUEs* and also guarantees certain minimum $SINR_{r,h}$ for *HIZUEs*. Our simulation results show that in comparison to the *Optimal Femto Power* (OptFP; Sathya et al., 2014) scheme (i.e., Femto transmits with optimal reduced power), it improves SINR of *IUEs* by 40%. However, the degradation in SINR of *IUEs* is only 1.6% when compared to the *Full Power Femto scheme*.

© 2015 Elsevier B.V. All rights reserved.

1 Introduction

The increased use of mobile devices has led to an increase in the demand for data services over cellular networks. This is partly addressed by intensifying the deployment of Macro Base Stations (MBSs) in the Long Term Evolution (LTE) cellular networks. The mobile operators can boost data rates for outdoor user equipments (*OUEs*) but are not able to increase the data rates for indoor user equipments (*IUEs*). This is because it is difficult for electromagnetic signals to penetrate through walls and floors. Thus, the *IUEs* suffer with low signal strengths. To demonstrate this, let us consider a single-floor building with a single MBS (interchangeably used as Macro in rest of this paper) placed at a distance of 350 m [2] on the south west side of the building. By taking into account path

losses due to walls and floors, the region up to which the signal from MBS can penetrate into the building is then measured and shown in Fig. 1. This figure shows the radio environmental map (REM) of the building where Z-axis is used to list out signal to noise ratio (SNR) values at various sub-regions (X, Y) inside the building. Owing to the walls inside the building, *IUEs* on average receive low SNR (e.g., -8 dB, -9 dB) compared to *OUEs* (e.g., 4 , 2 , 0 , -1 dB).

Cisco VNI Mobile Forecast [3] (2014–2019) tells that although only 3.9% of mobile connections were LTE based they accounted for 40% of the mobile traffic and this will rise to 51% by 2019, by which the mobile data usage will grow 11 fold to over 15 exabytes per month. Reports by Cisco and Huawei [4] tell that 70% of the traffic is caused by indoor users (*IUEs*). Hence, it is very important for telecom operators to improve coverage of indoor areas and boost data rates of *IUEs*. To achieve this, one can deploy a large number of low power nodes (LPNs) a.k.a. small cells (e.g., Picos and Femtos [5]) under an umbrella MBS coverage and thereby form an LTE heterogeneous network (HetNet). This increases spectrum

* Corresponding author. Tel.: +91 7382365762.
E-mail addresses: cs11p1003@iith.ac.in, vanlins8@gmail.com (V. Sathya), me11b005@iith.ac.in (A. Ramamurthy), ee13b1025@iith.ac.in (S. Sandeep Kumar), tblr@iith.ac.in (B.R. Tamma).

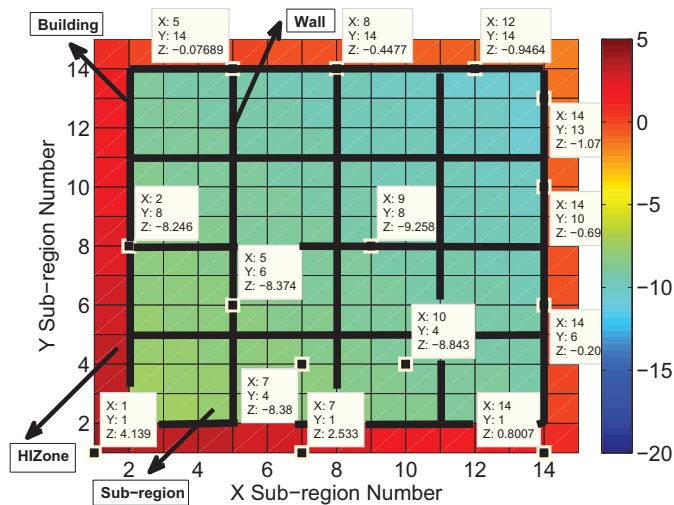


Fig. 1. REM of sub-regions inside building without any Femto cells deployed indoor.

efficiency by allowing spatial reuse of the same spectrum. Small cells can be installed by end users in residences and in large office environments and hotspots. But, co-tier interference among Femtos can occur, if they are placed arbitrarily and the operator tries to reuse the same spectrum, which would decrease the system capacity. In order to make the usage of spectrum more efficient for *IUEs*, placement of Femtos needs to be optimal. Optimal placement of Femtos ensures good *SINR* and thereby improves system capacity. In this work, we apply the Minimize Number of Femtos (*MinNF* [1]) model (explained in detail in Section 4) to determine the optimal count and the optimal placement of Femtos and hence reduces operator's CAPEX and OPEX. Hence, we expect that large scale enterprises could benefit from *MinNF* model based deployment. However, in some scenarios, operator's may need to go for sub-optimal or arbitrary deployment (due to physical constraints) which will lead to deployment of more number of Femtos than that in *MinNF* to ensure that there are no coverage holes. Even optimal placement of Femtos inside a building leads to power leakage at the edges/corners of the building. This degrades the performance of the *OUEs* (i.e., Macro connected) in high interference zone (*HIZone*) around the building area because both Macros and Femtos operate at the same frequency due to reuse one in LTE HetNets. In our work we specifically refer the *OUEs* in *HIZone* as *HIZUEs*.

To guarantee certain minimum *SINR* to both *IUEs* and *HIZUEs*, we apply the concept of device to device (*D2D*) communication in LTE HetNets. In *D2D*, devices (i.e., *UEs*) communicate directly with each other while the serving BS assists in setting up of *D2D* links and managing the control plane, authentication, handovers, etc. *D2D* helps in improving the cellular network capacity and power efficiency. In our work, we make use of idle *IUEs* as relays between Femtos and *HIZUEs* through *D2D* as an underlay to the LTE HetNet. We formulate a Mixed-Integer Linear Programming (*MILP*) model that chooses *D2D* pairs, and assigns radio resources and transmission power to each of *D2D* pairs. To reduce the time complexity, we propose a two-step heuristic algorithm. In step one, we find the sub-optimal *D2D* pairs and assign the radio resources for them. In step two, a Linear Programming (*LP*) model is used to determine the transmit power for *D2D* pairs.

Table 1 shows notations used in this work. Rest of the paper is organized in the following manner. Section 2 describes the related research works. Proposed LTE HetNet system architecture with *D2D* links is presented in Section 3. In Section 4, proposed placement *MILP* model which minimizes number of Femtos to be deployed,

Table 1
Notations used in our work.

Notation	Abbreviations
<i>D2D</i>	Device-to-device
<i>HIZUE</i>	<i>OUE</i> in <i>HIZone</i>
<i>HIZone</i>	High interference zone
<i>IUE</i>	Indoor UE
<i>LPN</i>	Low power node
<i>LP</i>	Linear Programming
<i>MBS</i>	Macro Base Station
<i>MILP</i>	Mixed Integer Linear Programming
<i>MinNF</i>	Minimize the Number of Femtos
<i>OptFP</i>	Optimal Femto Transmission Power
<i>PRS</i>	Position Reference Signal
<i>RB</i>	Resource block
<i>SINR</i>	Signal-to-interference plus noise ratio
$SINR_{th}$	Threshold <i>SINR</i>
<i>SON</i>	Self Organizing Network
<i>UE</i>	User Equipment

D2D *MILP* model and *D2D* heuristic algorithm are discussed. Performance results are explained in Section 5. Finally, Section 6 contains concluding remarks.

2. Related research work

Many approaches to placing Femtos have been discussed in literature with sufficient insight, keeping in mind various parameters such as building dimensions, interference from Macro BSs and other Femto BSs. In [6], small cell locations are optimized in an airport environment depending upon the traffic demand. In [7,8], Guo et al. suggested an automated small cell deployment model which attempts to find the optimal location of a new cell, subject to knowledge about the locations of existing cells, *UEs* and the building environment. A closed-form equation is given for the new cell's deployment location which is a function of transmit power, transmission scheme and path loss parameters. In [9], the authors investigated a joint Femto placement and power control optimization problem in enterprise buildings with the aim to prolong *UEs'* battery life. They proposed a novel two-step reformulation approach to convert the original mixed-integer non-convex problem (*MINCP*) into a *MILP* and then devised a global optimization algorithm by utilizing the *MILP*. But their system model did not consider co-tier and cross-tier interferences. In [10], Femtos are optimally placed in a multi-story enterprise building by not considering co-tier and cross-tier interferences. In [11], the authors proposed an iterative algorithm for optimizing deployment locations of cells based on a novel utility function (i.e., area proportional fairness utility which accounts for both user distribution and fair resource allocation) while accounting for mutual interference. Authors in [12] proposed an algorithm which gives the optimal transmission power of each of the Femtos deployed in a HetNet scenario by guaranteeing $SINR_{th}$ for *IUEs* and lesser degradation for *HIZUEs*. However, Femto power adaptation has not factored in occupancy level of *HIZUEs* outside the building.

In one of our previous works [13], an optimization problem is formulated for Femtos deployment which guarantees $SINR_{th}$ inside the building by considering co-tier interference, cross-tier interference and impedance caused by walls. We also varied the $SINR_{th}$ depending on average user density in each region inside the building. This resulted in improving spectral efficiency of Femtos deployed in indoors. However, *HIZUEs* suffered degradation in *SINR* due to cross-tier interference between Macros and Femtos. In [1], optimal placement of Femtos and dynamic control of their transmit powers are studied by solving two optimization models, namely *MinNF* and *OptFP*. *MinNF* determines the minimum number of Femtos

121 and their respective coordinates to guarantee a minimum $SINR_{th}$
 122 of 0 dB for all indoor regions, assuming full transmission power of
 123 the Femtos. Configuration of Femtos at the full transmission power
 124 degrades $SINR$ values of $HIZUEs$. To address this issue, OptFP model
 125 is used to find the optimal power of the Femtos to reduce degrada-
 126 tion in $SINR$ for the $HIZUEs$. The maximum fall in $SINR$ for $HIZUEs$ is
 127 limited to 2 dB after the deployment of Femtos. Since Femto power
 128 is reduced, $SINR_{th}$ of $IUEs$ is also reduced to -2 dB. This optimal
 129 power dynamically changes according to the occupancy of $HIZUEs$
 130 in the $HIZone$. But the presence of even a single $HIZUE$ decreases
 131 $SINR$ of numerous $IUEs$, which is not fair to $IUEs$. To ensure fair-
 132 ness for $IUEs$ and $HIZUEs$, we apply the concept of device-to-device
 133 (D2D) communication in this work.

134 D2D is one of the most promising and challenging aspects to-
 135 ward 5G. In D2D communication, two UEs communicate directly
 136 with each other by means of data plane (D-plane) transmission us-
 137 ing E-UTRA technology [14,15]. BS controls and optimizes the use
 138 of shared radio resources for cellular and D2D sessions. D2D is
 139 standardized by 3GPP in Rel-12 for proximity-based services [16].
 140 Some of the challenges in D2D include interference management,
 141 resource allocation, power control, session management, mobil-
 142 ity management, security, location estimation and multi-hop D2D
 143 [17–19]. Session management [20,21] in D2D is controlled by BS.
 144 Core network is used for authentication, control channel establish-
 145 ment and policy control. Authors of [22] proposed a resource al-
 146 location scheme to share resource blocks (RBs) among D2D pairs
 147 and traditional cellular users. In [23], the authors proposed an
 148 accurate model of the system and applied approximate dynamic
 149 programming model to do a fast resource scheduling in a Het-
 150 Net system with D2D support. In [24] Phantom cell concept (UE-
 151 like BS) was proposed as a solution using D2D links to offload
 152 the traffic but different frequencies for the C-plane and D-plane
 153 were used. In [25], a holistic approach to efficiently offload with
 154 D2D was proposed and it incorporated a two-time scale schedul-
 155 ing solution with joint uplink and downlink scheduling between
 156 D2D pairs. It was shown that reuse of spectrum using Fractional
 157 Frequency Reuse (FFR) is limited but has not adapted any dynamic
 158 power control in the solution. In [26], the authors studied different
 159 techniques to expand the cell edge coverage. They showed that us-
 160 ing D2D for cell edge users decreases the overall power consump-
 161 tion. Authors of [27] proposed an optimization problem based on
 162 practical link data model with the objective of minimizing power
 163 consumption while meeting user data requirements. To solve it in
 164 a polynomial time, the authors proposed a joint mode selection,
 165 channel allocation and power assignment for D2D pairs by using a
 166 heuristic algorithm, but they predetermined and fixed the number
 167 of D2D pairs.

168 Multi-hop D2D communication [28–30] is one of the most
 169 promising technologies in LTE used for military communication
 170 and disaster management. The two-hop or multi-hop can be ap-
 171 plied to the problem where the UE with poor direct link to the
 172 MBS will forward data to a nearby UE over a high quality D2D link
 173 in uplink communication [31]. Here the receiving UE uploads its
 174 own data and relayed data to the MBS over its good uplink. This
 175 decreases the transmission time of the UE when compared to poor
 176 direct link to the MBS. Similarly, other work in uplink communi-
 177 cation [32] describes the multi-hop D2D networking and resource
 178 management scheme for M2M communication to enhance end-to-
 179 end connectivity in an LTE network. In [33], the authors have pro-
 180 posed a novel distributed utility function for maximizing the D2D
 181 power control scheme which enables to balance spectral efficiency
 182 and resource allocation constraints that are essential in a given in-
 183 tegrated cellular-D2D environment. During mode selection the im-
 184 pact of interference with other devices has not been considered.
 185 Also it is to be noted that the allocation of resources are random,
 186 which leads to inefficient D2D pairing.

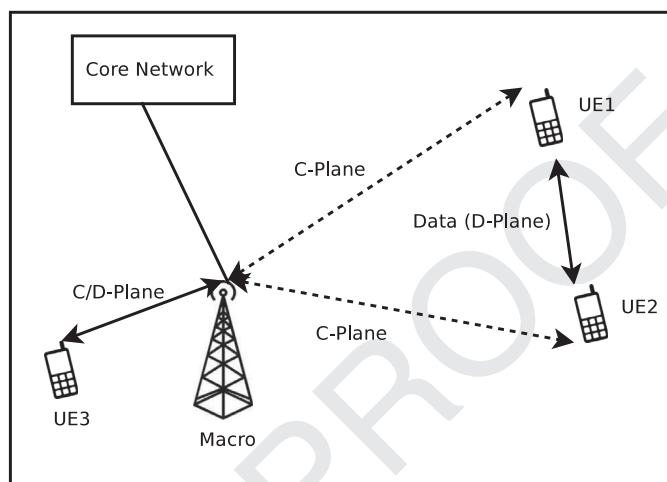


Fig. 2. Architecture of HetNet system with traditional and D2D links.

2.1. Our contributions

187
 188 In this work, we have considered obstacles (walls and floor) present
 189 inside buildings, and co-tier and cross-tier interference in LTE HetNets.
 190 We use MinNF MILP model (referred henceforth as MinNF) to guarantee
 191 $SINR_{th}$ for $IUEs$. In MinNF model, Femtos transmit with full power
 192 which could degrade the performance of $HIZUEs$. In order to ensure
 193 fairness and improve achievable data rates for both $IUEs$ and $HIZUEs$,
 194 we apply the concept of D2D communication wherein $IUEs$ act like
 195 UE-relays (i.e., UE-like BS, forwarding data-plane traffic for some of
 196 the outdoor UEs). We first formulate a D2D MILP model to guarantee
 197 a certain $SINR_{th}$ for both $IUEs$ and $HIZUEs$. To reduce the computa-
 198 tion time, we propose a two-step heuristic algorithm. In step one (called
 199 as hDPRA), we efficiently choose the potential D2D based relay pairs
 200 and allocate radio resources to them. In step two (called as hDPA), an
 201 LP model is formulated for power control of D2D links. We have con-
 202 ducted extensive evaluations to show that our proposed D2D heuristic
 203 algorithm is very close to the D2D MILP model.
 204

3. Proposed LTE HetNet system with D2D relays

205
 206 In this section, we present architecture of LTE HetNet system with
 207 D2D relays, system model, building model and channel model.
 208

3.1. HetNet architecture with D2D relays

209
 210 In traditional cellular networks, UEs communicate with each other
 211 only through BSs (e.g., Macros, Picos, and Femtos). But in D2D [18],
 212 UEs communicate directly with each other for exchanging data traffic
 213 (D-plane) and the serving BS only assists in the establishment and
 214 maintenance of D2D links as shown in Fig. 2. In our HetNet archi-
 215 tecture with D2D relays, Femtos make use of free/idle $IUEs$ (FIUEs)
 216 in their cells as UE-relays for forwarding downlink data traffic (D-
 217 plane) of $HIZUEs$ by setting up D2D links (i.e., $FIUE \rightarrow HIZUE$).
 218 Hence, $HIZUEs$ are going to be served in downlink by one of Fem-
 219 tos deployed inside the building by using FIUEs (typically located at
 220 Femto cell-edge regions) as relay nodes. However, $HIZUEs$ always
 221 communicate with MBS for their uplink communication. The control
 222 traffic (C-plane) for the $HIZUEs$ is still delivered by the MBS [15]
 223 for better reliability and reducing the number of handovers for
 224 $HIZUEs$ which are typically more mobile than indoor UEs.
 225

226 The architecture of proposed HetNet system with D2D based relays
 227 is shown in Fig. 3. The data traffic (D-plane) for the $HIZUEs$

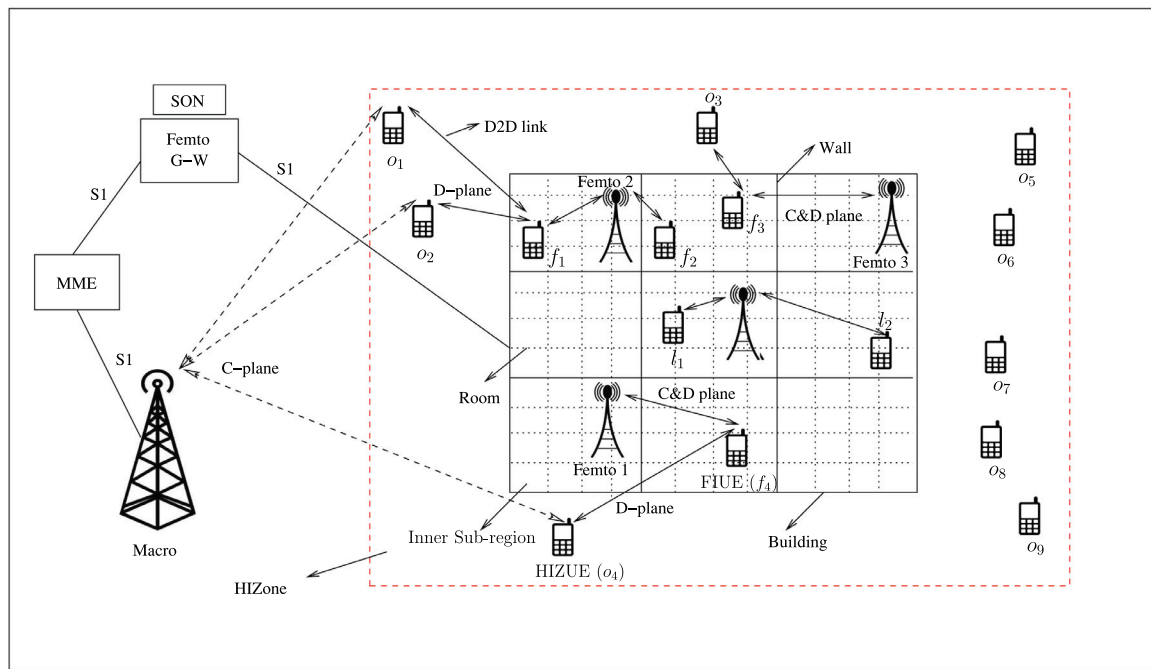


Fig. 3. Architecture of proposed HetNet system with D2D based relays.

is first sent to FIUEs from the Femto by normal cellular communications. The FIUEs act as UE-relays and forward the data traffic to the HIZUEs. All the Femtos are connected to a Femto-Gateway (F-GW) over S1 interface. Self Organization Network (SON) features (e.g., optimally choosing D2D links and tuning their transmit power levels) can be integrated into the F-GW to automate the network operation. Broadly there are two approaches for choosing D2D links and fine tuning of their transmit power levels: distributed one which could be implemented at FIUEs and centralized one which could be implemented at the F-GW/SON. Both these approaches require the knowledge of distance/channel state information between FIUEs and HIZUEs for establishing D2D links with the required transmit power. But, it is very challenging and costly to acquire this information at FIUEs and choose D2D links by themselves in a distributed manner. Hence, in our work, we consider the centralized approach (i.e., Network assisted mode [34,35]) by implementing the proposed D2D heuristic algorithm at the F-GW/SON. MBS periodically provides the list of potential HIZUEs (through C-plane messages) to the F-GW/SON. Femtos also provide the list of potential FIUEs to the F-GW/SON periodically (e.g., 10 ms which is equal to one LTE frame duration). The downlink channel (from FIUEs to HIZUEs) quality can be estimated at HIZUEs by overhearing the uplink sounding reference signals (SRSS [16,36–38]) of the FIUEs. Note that SRSSs are sent periodically by FIUEs in the uplink to the serving Femtos for estimating uplink channel state. HIZUEs listening to these SRSSs could estimate their downlink channel state and convey the same to F-GW/SON via MBS. If FIUEs are configured not to send SRSSs, then the F-GW/SON needs to go for default power setting for D2D links. The D2D heuristic algorithm which is implemented at the F-GW/SON determines D2D links and their respective transmit power levels for communicating the same to respective FIUEs via their respective serving Femtos.

The D2D connection setup process involves choosing one of the FIUEs as UE-relay through D2D candidate indication message sent from the corresponding Femto via F-GW (refer Fig. 4). Similarly the same D2D candidate indication message sent from MBS via F-GW informs the corresponding HIZUE. The FIUE and HIZUE then initiate the D2D connection setup procedure [39,40] by sending ACK from

FIUE to F-GW via Femto. Similarly, once the ACK sent from HIZUE to F-GW via MBS. After D2D connection setup is established, D2D data transfer (D-Plane) procedure will take place.

3.2. System model

In this work, we consider an LTE HetNet system of MBSs in outdoor environment, to which the OUEs are associated, and Femtos inside an enterprise office building as shown in Fig. 3. We have considered the case where Femtos and MBSs operate on the same frequency band (i.e., reuse of one) to improve system's capacity. But, this can lead to high co-channel interference and affect HIZUEs' performance. We also assume that Femtos are all configured in open access i.e., UEs are authorized to connect with any of the Femtos of an operator. IUEs are connected to one of the Femtos deployed inside the building. There are two types of IUEs: legacy IUEs (LIUEs) represented by $l_1, l_2, l_3, \dots, l_m$ and free/idle IUEs (FIUEs) represented by $f_1, f_2, f_3, \dots, f_n$ as shown in Fig. 3. HIZUEs are represented by $o_1, o_2, o_3, \dots, o_p$. LIUEs are IUEs who send/receive data to/from a Femto at a particular Transmission Time Interval (TTI) for their own communication. FIUEs are IUEs who can act as UE-relays between their respective serving Femtos and one of HIZUEs. FIUEs can either be idle UEs or the UEs who are not going to be scheduled to receive any downlink data of their own from their serving Femtos for some TTIs. We assume that list of FIUEs is available at the F-GW/SON and it is updated dynamically.

The default scheduling algorithm is assumed to be running at each Femto for serving IUEs. The scheduling for downlink data of HIZUEs connected using D2D relays is also done at the Femtos. The D2D pairs are chosen such that they could be held for quiet sometime, so they will not be changing in every TTI. This can be assured if appropriate D2D Device Discovery mechanism [41] is used for choosing the FIUEs. We assume that the transmission power across resource blocks (RBs) for the Femtos are equal whereas for that of the FIUEs the power is varied accordingly to each RB. The D2D based relays (FIUEs) do not face severe battery issues because the FIUEs transmit at lower power. The FIUEs can also be provided with incentives by the operator for acting as D2D based UE-relays.

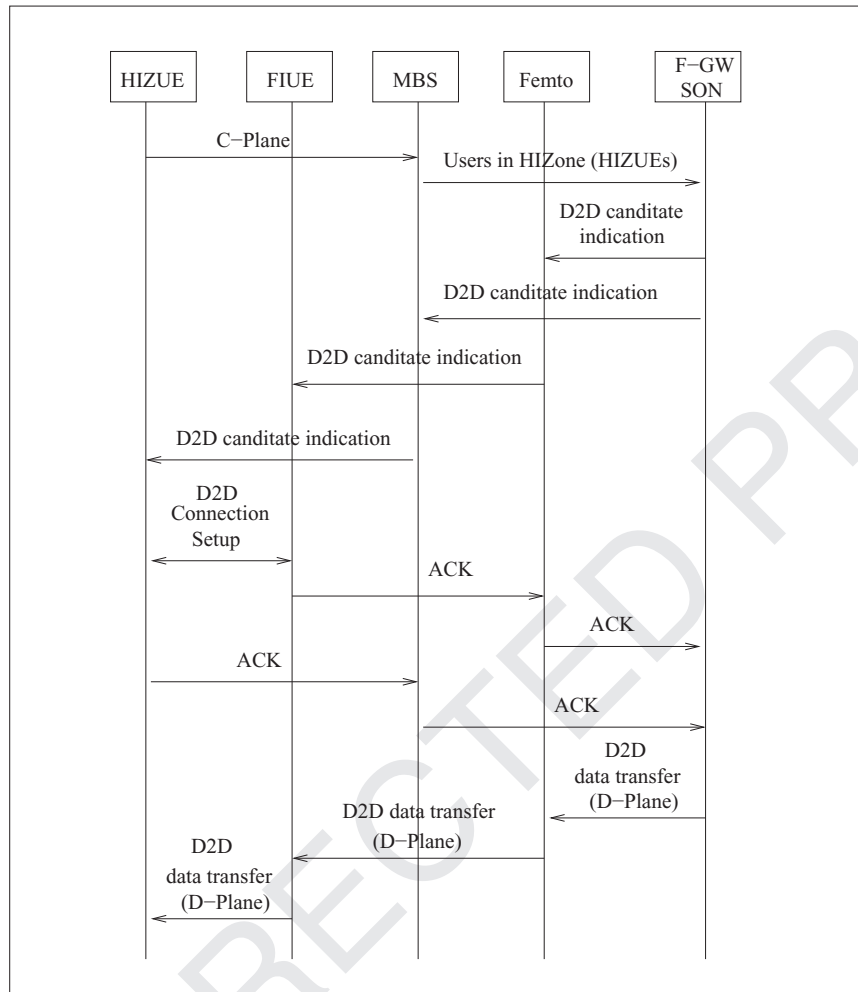


Fig. 4. Call flow diagram for D2D based communication in proposed HetNet system.

302 A variety of scenarios can co-exist in this HetNet system model
 303 for the D2D links as shown in Fig. 3. A D2D link can be established
 304 by an FIUE to serve one or more HIZUEs. A single FIUE can also
 305 serve multiple HIZUEs using D2D links. In the worst case, when
 306 it is impossible to establish any D2D link due to high load at the
 307 Femto or lack of FIUEs, the F-GW/SON can opt for *dynamic Femto*
 308 *power (OptFP)* model [1] in order to reduce interference to HIZUEs
 309 from the Femtos (explained later in Section 4.4).

310 3.3. Building model

311 Consider the dimensions of a building to be $L \times W \times H$, where
 312 L , W and H are respectively the length, width and height. Each
 313 floor is divided by walls into several rooms as shown in Fig. 3.
 314 Each room is further logically divided into smaller inner sub-
 315 regions, S_i s. For example, a building which is divided logically into
 316 $(I_1, I_2, \dots, I_{144})$ is shown in Fig. 5. The thick lines represent the
 317 walls of the rooms and the small squares are the sub-regions. Sim-
 318 ilarly, the HIZone region outside the building is divided into outer
 319 sub-regions, S_o s. In the example, they are O_1, O_2, \dots, O_{52} . As the
 320 size of sub-region is much smaller compared to the building/room
 321 size, we can safely assume that within every sub-region, the aver-
 322 age SINR value is almost constant.

323 3.4. Channel model

324 The Path Loss (PL) between MBS and IUEs or HIZUEs is given
 325 by [12]:

$$PL_{macro} = 40 \log_{10} \frac{d}{1000} + 30 \log_{10} f + 49 + n\phi \quad (1)$$

326 where, d is the distance of the IUE/HIZUE from MBS in meters, n is
 327 the number of walls in between MBS and IUE/HIZUE, f is the center
 328 frequency of MBS and ϕ is the penetration loss of a wall. To
 329 account for the fact that Femtos are placed in a multi-story build-
 330 ing, PL between Femto and IUE/HIZUE is given by:

$$PL_{femto/D2D} = 37 + 30 \log_{10} d + 18.3v^{\frac{(v+2)}{(v+1)-0.46}} + n\phi \quad (2)$$

331 where v is the number of floors in between Femto and IUE/HIZUE.
 332 We assume that PL model for D2D links is same as that of between
 333 Femto and IUE/HIZUE. We also assumed that the antenna gain for
 334 Macros and Femtos are 20 dBi and 2 dBi, respectively. We calculate
 335 the channel gain between UEs and various BSs using the PL models
 336 given above and antenna gains [42].

337 4. Femto placement and D2D pair selection models in LTE 338 HetNets

339 In this section, we first present Minimize the Number of Fem-
 340 tos (MinNF) MILP model for determining the number of Femtos
 341 to be deployed in LTE HetNet system. Then we formulate D2D
 342 MILP model which establishes D2D based relay pairs between FI-
 343 UEs and HIZUEs and also guarantees certain SINR threshold ($SINR_{th}$)
 344 for both IUEs and HIZUEs. As D2D MILP model takes more compu-
 345 tation time, it is not usable in real-world deployments for estab-
 346 lishing D2D pairs dynamically. To address this issue, we propose a
 347 two-step heuristic algorithm for establishing D2D pairs.

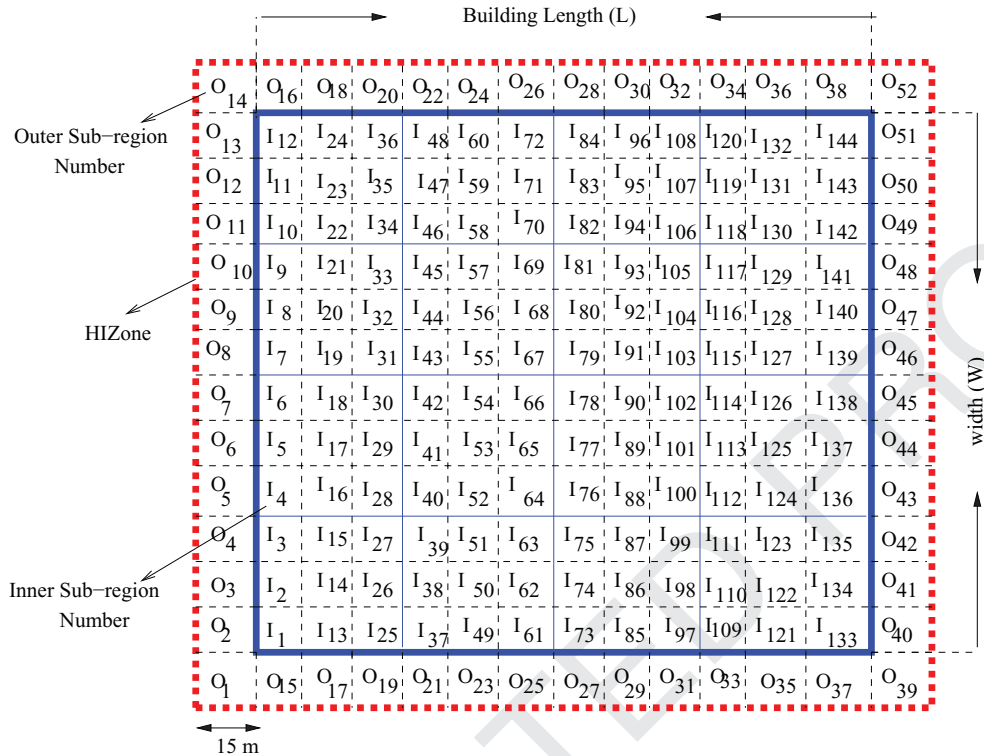


Fig. 5. Bird-eye view of floor area inside and outside a single-floor building.

Table 2
Glossary of MinNF MILP Model.

Notation	Definition
S_i	Set of all inner sub-regions
S_o	Set of all outer sub-regions
w_a	1 if Femto is placed at inner sub-region a, zero otherwise
y_{ja}	1 if j th inner sub-region of the building is associated with the Femto located at inner sub-region a, zero otherwise
G_{ja}	Channel gain between inner sub-regions j and a
M	Set of all MBSs

deployed, expressed by Eq. (3).

$$\min \sum_{a \in S_i} w_a \quad (3)$$

Every sub-region (i.e., all IUEs present in a sub-region) is allowed to associate with only one Femto BS (refer Eqs. (4) and (5)) inside the building.

$$\sum_{a \in S_i} y_{ja} = 1 \quad \forall j \in S_i \quad (4)$$

$$y_{ja} - w_a \leq 0 \quad \forall j, a \in S_i \quad (5)$$

MinNF model needs to guarantee a certain minimum $SINR_{th}$ for all IUEs present in every sub-region of the building. The L.H.S. of the Eq. (6) is the SINR received by a particular inner sub-region j from the Femto located at sub-region a based on the worst case assumption of using all the resource blocks by all Femtos and MBS in the HetNet system. To ensure good coverage, the SINR received in each of inner sub-regions must be maintained above the predefined threshold λ (which is the $SINR_{th}$), given by:

$$\frac{Inf * (1 - y_{ja}) + G_{ja} P_{max}^f w_a}{N_0 + \sum_{b \in S_i \setminus a} G_{jb} P_{max}^f w_b + \sum_{e \in M} G_{je} P_{macro}} \geq \lambda \quad \forall j, a \in S_i \quad (6)$$

The above Eq. (6) can be rewritten as,

$$Inf * (1 - y_{ja}) + G_{ja} P_{max}^f w_a \geq \left(\lambda N_0 + \sum_{b \in S_i \setminus a} G_{jb} P_{max}^f w_b \lambda + \sum_{e \in M} G_{je} P_{macro} \lambda \right) \quad \forall j, a \in S_i \quad (7)$$

G_{je} and G_{ja} are the channel gain from Macro and Femto calculated using Eqs. (1) and (2), respectively, N_0 is the system noise and P_{macro} is the Macro BS's transmission power. In Eq. (6), Inf is a virtually infinite value (a very large value like 10^6). The reason for using $Inf * (1 - y_{ja})$ is that if $y_{ja} = 0$ then $Inf * (1 - y_{ja})$ becomes a large value and the expression can be ignored safely. Without

4.1. Femto placement: minimize the number of Femtos (MinNF) MILP model

In MinNF model, the minimum number of Femtos required for placement inside a building to provide a threshold SINR ($SINR_{th}$) to every inner sub-region is estimated. The aim is to boost the average SINR for all the IUEs by deploying optimal number of Femtos and maintain a minimum $SINR_{th}$ in all the inner sub-regions. To boost the data rate for IUEs, the Femtos that transmit at the peak power must be placed optimally inside the building without any coverage holes. The objectives of the MinNF model are given below:

- Minimize the number of Femtos, NF_{min} , needed for maintaining certain $SINR_{th}$ in each inner sub-region of the building.
- Determine the optimal locations for placement of NF_{min} Femtos inside the building.
- Identify the Femtos in NF_{min} to which the IUEs have to be associated.

The MinNF method has been described below and Table 2 shows the notation used in MinNF model. In order to provide a good SINR to IUEs, every Femto operates at its peak transmit power (P_{max}^f). The goal is to minimize the total number of Femtos

Table 3
Glossary of D2D MILP Model.

Notation	Definition
K	Set of all resource blocks (RBs)
F	Set of all Free Indoor UEs (FIUEs)
L	Set of all Legacy Indoor UEs (LIUEs)
O	Set of all Outdoor UEs in HIZone (HIZUEs)
M	Set of all MBSs
D_{fo}	A binary variable whose value is 1 if f is connected to o for D2D else 0, where $f \in F, o \in O$
C_{fo}^k	A binary variable whose value is 1 if f is connected to o for D2D using RB k else 0, where $f \in F, o \in O, k \in K$
h_f^k	A binary variable whose value is 1 if f is using RB k for D2D link else 0, where $f \in F, k \in K$
G_{xy}	Channel gain between two nodes x and y , where nodes can be FIUEs, HIZUEs, MBSs or Femtos
p_f^k	Normalized power emitted by f in RB k , $0 \leq p_f^k \leq 1$, where $f \in F, k \in K$

389 the virtual infinite value, Eq. (6) ensures that all the Femtos provide a minimum $SINR_{th}$ to a particular sub-region. But just a single
390 Femto is necessary to give $SINR_{th}$ for any given inner sub-region.
391 The proposed MILP model will always be infeasible if we do not
392 use the virtual infinite value as not all Femtos can meet $SINR_{th}$ in
393 each inner sub-region. Finally, the MinNF model is formulated as
394 follows,
395

$$396 \quad \min \sum_{a \in S_i} w_a \quad \text{s.t. (4), (5), (7).}$$

397 As shown later in Section 5, the proposed MinNF model guar-
398 antees that with minimum number of Femtos, all users inside the
399 building get a certain $SINR_{th}$ (λ). It is a reasonable approach to
400 boost the indoor SINR as the Femtos transmit at their maximum
401 transmission power. Since Femtos and Macros operate on the same
402 spectrum band, interference can occur between the Femtos and
403 Macro users and it in turn would degrade the signal strength of the
404 HIZUEs in HIZone. To avoid the degradation of HIZUEs and to guar-
405 antee certain minimum SINR for both FIUEs and HIZUEs, we propose
406 another optimization model, in next section, that optimally selects
407 D2D links between FIUEs and HIZUEs to maintain $SINR_{th}$ for both
408 FIUEs and HIZUEs.

409 4.2. D2D MILP model

410 In order to achieve the required $SINR_{th}$ for both FIUEs and HIZUEs
411 in the HetNet system, we need to optimally choose D2D links, ef-
412 fectively allocate the RBs to the D2D links and adjust power for
413 these links. We formulate a MILP model to address this problem.
414 The notations used in this model are listed in Table 3.

415 In order to minimize battery drain of FIUEs, one of the main
416 objectives¹ is to minimize the overall power consumed by the D2D
417 links as expressed in Eq. (8):

$$418 \quad \min \sum_{f \in F} \sum_{k \in K} p_f^k \quad (8)$$

419 Eq. (9) sets an upper bound on the number of HIZUEs that can be
420 served by each FIUE. Similarly, Eq. (10) restricts the number of FI-
421 UEs serving each HIZUE.

$$421 \quad \sum_{o \in O} D_{fo} \leq \alpha \quad \forall f \in F \quad (9)$$

$$422 \quad \sum_{f \in F} D_{fo} \leq \beta \quad \forall o \in O \quad (10)$$

¹ Another alternate optimization goal can be minimization of the maximum power ($\min(\max(p_f^k))$) consumed by D2D links where all the constraints are identical to the proposed D2D MILP model.

$$\sum_{f \in F} \sum_{o \in O} D_{fo} = \psi \quad \forall o \in O \quad (11)$$

423 In order to limit the total number of D2D links that would be
424 established in a TTI, we introduce Eq. (11). The values of α , β and
425 ψ can be fine tuned as per the requirements of the operator. The
426 binary variable C_{fo}^k is 1 when FIUE f and HIZUE o are communi-
427 cating by using RB k . Hence, C_{fo}^k can never be 1 when there is no
428 D2D link between f and o . This is ensured by Eq. (12). Here, η rep-
429 resents the maximum number of RBs that can be assigned to each
430 D2D link.

$$\sum_{k \in K} C_{fo}^k \leq \eta \times D_{fo} \quad \forall f \in F, o \in O \quad (12)$$

431 Eq. (13) ensures that the maximum number of times a particu-
432 lar RB k can be reused by an FIUE f is 1.

$$\sum_{o \in O} C_{fo}^k \leq 1 \quad \forall f \in F, k \in K \quad (13)$$

433 h_f^k is set to be 1 if FIUE f is using the RB k . This is ensured by Eq.
434 (14).

$$435 \quad h_f^k = C_{fo}^k \quad \forall f \in F, o \in O, k \in K \quad (14)$$

436 The constraint in Eq. (15) ensures that the normalized power
437 emitted by FIUE f in a particular RB k is 0 when it is not used by f .

$$438 \quad p_f^k \leq h_f^k \quad \forall f \in F, k \in K \quad (15)$$

439 The P_{max}^d is the maximum power of a D2D link. Once the MILP
440 model is solved, transmission power of an FIUE f in a RB k is cal-
441 culated as $p_f^k \times P_{max}^d$. G_{fl} gives the gain from the FIUE f to the LIUE
442 l . S_l^k is an input parameter whose value is 1 when l is connected
443 to its serving Femto (downlink) using RB k , else 0. The constraint
444 in Eq. (16) ensures that the maximum interference power that is
445 received by l is less than the allowed threshold value (I_l). I_l is com-
446 puted for a given value of $SINR_{th}$ of FIUEs.

$$447 \quad \sum_{f \in F} (G_{fl} \times S_l^k \times p_f^k \times P_{max}^d) \leq I_l \quad \forall l \in L, k \in K \quad (16)$$

448 The L.H.S. of Eq. (17) is the SINR received by HIZUE o from FIUE
449 f . To ensure good connection, the SINR of each D2D link is main-
450 tained above a predefined threshold λ_o which could vary across
451 HIZUEs.

$$452 \quad \frac{Inf * (1 - C_{fo}^k) + G_{fo} p_f^k P_{max}^d}{N_o + \sum_{m \in M} G_{mo} P_{macro} + \sum_{a \in B_k} G_{ao} P_{max}^f + \sum_{f' \in F \setminus f} G_{fo'} p_{f'}^k P_{max}^d} \geq \lambda_o \quad (17)$$

453 Here, B_k is the set of all Femtos using the RB k in a given
454 TTI. Similarly, G_{ao} is the channel gain from Femto a to o , G_{fo} is
455 the channel gain from f to o and G_{mo} is the channel gain from
456 MBS m to o , calculated by using Eq. (1) or Eq. (2). The need to
457 use $Inf * (1 - C_{fo}^k)$ is that if $C_{fo}^k = 0$ then $Inf * (1 - C_{fo}^k)$ becomes a
458 large value and the expression can be ignored safely. Without the
459 virtual infinite value, Eq. (17), ensures that all the FIUEs provide
460 a minimum $SINR_{th}$ to a particular HIZUE. The MILP will always be
461 infeasible if we do not use the virtual infinite value, as not all FI-
462 UEs can maintain a $SINR_{th}$ (λ_o) for an HIZUE. The Eq. (17) can be
463 rewritten as follows,

$$464 \quad Inf * (1 - C_{fo}^k) + G_{fo} p_f^k P_{max}^d \geq \left\{ \left(\lambda_o N_o + \lambda_o \sum_{m \in M} G_{mo} P_{macro} \right. \right. \\ \left. \left. + \lambda_o \sum_{a \in B_k} G_{ao} P_{max}^f + \lambda_o \sum_{f' \in F \setminus f} G_{fo'} p_{f'}^k P_{max}^d \right) \right\} \quad \forall f \in F, o \in O, k \in K \quad (18)$$

Finally, the D2D MILP model is formulated as follows,

$$\min \sum_{f \in F} \sum_{k \in K} p_f^k s.t.,$$

(9), (10), (11), (12), (13), (14), (15), (16), (18).

By solving this MILP model, we achieve the following:

- Get best FIUEs as relays for establishing D2D links
- Assign RBs to each of the D2D links established
- Adjust the transmit power for each of the D2D links and minimize the overall power emitted by guaranteeing $SINR_{th}$ for LIUEs and HIZUEs served by FIUEs.

As shown later in Section 5, the above D2D MILP model ensures fairness for both indoor and outdoor users by assuring certain minimum $SINR$ for all IUEs and HIZUEs. But the computation time of this D2D MILP model is high so the solution will not converge in real-time for any practical usage by Femto cells. To overcome this shortcoming, we propose a two-step D2D heuristic algorithm in the next sub-section.

4.3. D2D heuristic algorithm

D2D heuristic algorithm has two steps: one step for selecting D2D pairs and allocating RBs, and other step for setting the powers of D2D pairs. Below we present these two steps.

Step 1: Heuristic D2D pair and resource allocation (hDPRA)

Proposed hDPRA (refer Algorithm 1) checks whether a particular FIUE f can connect to an HIZUE o using an RB k . For this we define a parameter, Win-to-Loss (W2L) Ratio (γ) for all possible (f, o, k) combinations, as expressed in Eq. (19).

$$\gamma_{fo}^k = \frac{G_{fo}}{\sum_{o' \in O_k} G_{fo'} + \sum_{l' \in L_k} G_{fl'} + \sum_{f' \in F_k} G_{f'o}} \quad (19)$$

Here, $O_k (\subset O)$ represents the set of HIZUEs receiving data using the RB k , $L_k (\subset L)$ represents the set of LIUEs receiving data from Femto using the RB k and $F_k (\subset F)$ represents the set of FIUEs transmitting data to HIZUEs using the RB k . The numerator in the R.H.S. of Eq. (19) represents the gain between f and o , so it acts as an approximate measure (since the transmission power is not considered) for signal strength. The values $G_{fo'}$, $G_{fl'}$ and $G_{f'o}$, in the denominator represent the channel gain between f and o' , f and l' , and f' and o , respectively and they act as an approximate measure of the interference caused by the interfering links. The numerator and denominator are two opposing parameters to the W2L ratio. Hence, larger the value of γ_{fo}^k , higher the possibility of the particular combination (f, o) to have a D2D link using RB k . W2L ratio will be higher in case RB k is not used by some Femtos for serving their UEs in a given TTI i.e., the value of $\sum_{l' \in L_k} G_{fl'}$ will reduce in Eq. (19).

σ^* is the set that contains the triplet (f^*, o^*, k^*) if f^* and o^* are having a D2D link using RB k^* . Every element in σ^* should have its W2L ratio greater than $\bar{\gamma}$, an operator defined parameter which gives control over the number of D2D links that can be formed. Initially σ^* is a null set. We start by computing the W2L ratio for each (f, o) pair for all possible RBs and store them in the γ matrix. From this set, the maximum W2L ratio is found and this gives the corresponding triplet ($f_{max}, o_{max}, k_{max}$). On adding this particular triplet to σ^* , there will be additional interference ($G_{f_{max}o^*}$) to the existing (f^*, o^*) pairs who are using RB k_{max} for their data transmissions. Hence, $\gamma_{f^*o^*}^{k_{max}}$ values have to be recalculated and checked whether they remain greater than $\bar{\gamma}$. If all of these values remain greater than $\bar{\gamma}$, the triplet ($f_{max}, o_{max}, k_{max}$) is added to σ^* and the recalculated $\gamma_{f^*o^*}^{k_{max}}$ values are stored in the γ matrix, otherwise triplet ($f_{max}, o_{max}, k_{max}$) is not added to σ^* . In case triplet ($f_{max},$

Algorithm 1 Heuristic D2D pair and resource allocation (hDPRA) algorithm.

Input 1 : F, O, L

Input 2 : Optimal Femto Locations (Obtained by solving MinNF model)

Input 3 : $\bar{\gamma}, \alpha$ and β values

Output : D_{fo}, C_{fo}^k, h_f^k

Initialization ();

1: $D_{fo} \leftarrow 0 \quad \forall f \in F, o \in O$

2: $C_{fo}^k \leftarrow 0 \quad \forall f \in F, o \in O, k \in K$

3: Compute $\gamma_{fo}^k \quad \forall f \in F, o \in O, k \in K$ and store in γ matrix

4: $\alpha_f \leftarrow 0 \quad \forall f \in F$ { Count for number of HIZUEs connected to each FIUE }

5: $\beta_o \leftarrow 0 \quad \forall o \in O$ { Count for number of FIUEs serving each HIZUE }

6: $\sigma^* \leftarrow \{ \}$

7: **while** $\text{size}(\gamma) \neq 0$ **do**

8: $(f_{max}, o_{max}, k_{max}) \leftarrow \max(\gamma)$;

9: **if** Updated W2L values of entries in $\sigma^* > \bar{\gamma}$ **then**

10: $D_{f_{max}o_{max}} \leftarrow 1$

11: $C_{f_{max}o_{max}}^k \leftarrow 1$

12: $\alpha_{f_{max}} ++$

13: $\beta_{o_{max}} ++$

14: **if** $\alpha_{f_{max}} == \alpha$ **then**

15: Remove $\gamma_{f_{max}o}^k \quad \forall o \in O, k \in K$

16: **end if**

17: **if** $\beta_{o_{max}} == \beta$ **then**

18: Remove $\gamma_{fo_{max}}^k \quad \forall f \in F, k \in K$

19: **end if**

20: Remove $\gamma_{f_{max}o_{max}}^{k_{max}}$

21: **if** Updated $\gamma_{fo}^{k_{max}} < \bar{\gamma}$ **then**

22: Remove $\gamma_{fo}^{k_{max}}$ {Removes all f and o pairs using RB k_{max} from γ matrix }

23: **end if**

24: $\sigma^* \leftarrow \sigma^* \cup (f_{max}, o_{max}, k_{max})$

25: **else**

26: Remove $\gamma_{f_{max}o_{max}}^{k_{max}}$

27: **end if**

28: **end while**

o_{max}, k_{max}) is added to σ^* , the $\alpha_{f_{max}}$ and $\beta_{o_{max}}$ values are incremented, where $\alpha_{f_{max}}$ is the count for the number of HIZUEs connected to FIUE f_{max} and $\beta_{o_{max}}$ is the number of FIUEs connected to HIZUE o_{max} . If $\alpha_{f_{max}}$ value reaches the maximum limit α , then all the γ_{fo}^k values for FIUE f_{max} are removed from the γ matrix. Similarly if $\beta_{o_{max}}$ reaches the maximum limit of β , then all the γ_{fo}^k values for HIZUE o_{max} are removed from the γ matrix. W2L ratio in the γ matrix is updated $\forall f, o$ which are using RB k_{max} . If any of the updated $\gamma_{fo}^{k_{max}}$ is lesser than $\bar{\gamma}$, then that value is removed from the γ matrix and is not considered during the next iteration. Finally, it removes $\gamma_{f_{max}o_{max}}^{k_{max}}$ from the γ matrix and continues to the next iteration until all the entries are removed from the γ matrix.

Step 2: Heuristic D2D power allocation (hDPA)

Using outputs of the hDPRA from the Step 1, namely D_{fo}, C_{fo}^k, h_f^k , as the input in the Step 2 we solve an LP model which adjusts the power for each of the D2D links. The LP model is formulated similar to D2D MILP model presented earlier but with fewer

534 constraints as given below.

$$\min \sum_{f \in F} \sum_{k \in K} p_f^k \quad (20)$$

$$535 \quad p_f^k \leq h_f^k \quad \forall f \in F, k \in K \quad (21)$$

$$536 \quad \sum_{f \in F} (G_{fl} \times S_{lk} \times p_f^k \times P_{max}^d) \leq I_l \quad \forall l \in L, k \in K \quad (22)$$

$$537 \quad \text{Inf}_f * (1 - C_{fo}^k) + G_{fo} p_f^k P_{max}^d \geq \left\{ \left(\lambda_o N_o + \lambda_o \sum_{m \in M} G_{mo} P_{macro} \right. \right. \\ \left. \left. + \lambda_o \sum_{a \in B_k} G_{ao} P_a^{fem} + \lambda_o \sum_{f' \in F \setminus f} G_{f'o} p_{f'}^k P_{max}^d \right) \right\} \quad \forall f \in F, o \in O, k \in K \quad (23)$$

538 Finally, the LP model for D2D power control is formulated as
539 follows,

$$\min \sum_{f \in F} \sum_{k \in K} p_f^k \text{ s.t.}$$

540 (21),(22), (23).

541 As shown later in Section 5, the proposed two-step D2D heuristic
542 algorithm is fair to both the IUEs and HIZUEs by choosing the
543 D2D links, allocating resources to the D2D links and adjusting their
544 transmission power levels. It runs in polynomial time (refer Ap-
545 pendix A) and its low running time makes it usable at F-GW/SON.

546 4.4. Optimal Femto transmission power (OptFP) MILP model

547 Under some circumstances, when it is not possible to establish
548 D2D links due to lack of FIUEs (for example: if we observe Fig. 3,
549 there are no FIUEs present in east side of the building to establish
550 D2D link with HIZUEs (o_5, o_6, o_7 and o_8)), the F-GW/SON can be di-
551 rected to reduce the Femto transmission power, thereby reducing
552 the interference to HIZUEs from it. The arbitrary tuning of Femto
553 transmit power may degrade the performance of total IUEs con-
554 nected to that Femto and also cause coverage issues. We propose
555 a means to optimally control the Femto transmit power whenever
556 there are HIZUEs present outside the building but no FIUE is in-
557 side, thereby guaranteeing a minimum $SINR_{th}$ for IUEs and reduce
558 the interference to HIZUEs. The corresponding HIZUE can then con-
559 nect with MBS for D-plane communication. We formulated this as
560 OptFP MILP model in [1] and by solving it we can,

- 561 • Determine the optimal power required by each Femto for main-
562 taining the $SINR_{th}$ in each of the inner sub-regions and maintain
563 the SINR degradation at less than 2 dB for HIZUEs.
- 564 • Determine the Femto to which the users in any given inner
565 sub-region have to be associated with.

566 4.5. Joint D2D heuristic and OptFP (JDHO) algorithm

567 In most of the cases, the S-GW/SON might not be able to estab-
568 lish D2D links in all sides of the building. It is also equally probable
569 that D2D links are established more readily in some sides of the
570 building and not in the other sides due to lack of FIUEs (for exam-
571 ple, east and west sides of the building given in Fig. 3). Hence, the
572 S-GW/SON has to reduce the transmit power of Femtos optimally
573 so as to allow the HIZUEs to connect with one of MBSs. This can
574 be achieved by the combinatorial utilization of both D2D heuristic
575 algorithm and OptFP model (called as JDHO algorithm), that would
576 allow some HIZUEs which do not have any FIUE to get connected
577 to one of MBSs and the remaining HIZUEs through D2D links. The
578 proposed JDHO algorithm is given in Algorithm 2.

Algorithm 2 Joint D2D Heuristic and OptFP (JDHO) algorithm.

Input 1 : Set of all inner and outer sub-regions

Input 2 : Potential HIZUEs in HIZone

- 1: All Femtos are configured to transmit at their peak power by default.
- 2: All HIZUEs (O) are connected to one of MBSs for their C-Plane.
- 3: Find the set of all HIZUEs, O' , for whom it is not possible to establish D2D based relays by using FIUEs. $O' \subset O$.
- 4: Find the set of Femtos, B' , who are causing interference to O' HIZUEs. $B' \subset B$.
- 5: Apply the OptFP model [1] on B' to reduce their transmit powers so that interference to O' is reduced.
- 6: The O' HIZUEs are then allowed to connect to one of MBSs even for their D-plane (i.e., no D2D links, it is the traditional cellular communication).
- 7: Apply D2D Heuristic Algorithm (Algorithm 1) on $(O - O')$ HIZUEs to establish D2D based relays by using FIUEs

546 4.6. Cost analysis 579

580 In our system model, two-hop communication cost is essen-
581 tially the additional resources incurred by the proposed system
582 over the existing traditional system. It can be classified as resource
583 utilization, energy consumption and additional interference due to
584 the reuse of spectrum.

- 585 1. **Resource utilization:** In the first-hop communication (Femto to
586 LIUEs/FIUEs), the radio resources (RBs) allocated for the data
587 demanded by HIZUEs are the additional cost incurred by the
588 proposed system. If the downlink scheduler at the Femto has
589 excess resources (even after fulfilling the demand of the IUEs
590 in a TTI) then the additional cost incurred is zero. But, if the
591 Femto lacks excess resources, then the cost to the system is
592 the resources allocated to the FIUEs to receive HIZUEs data from
593 the Femto. These resources could have otherwise been sched-
594 uled to the LIUEs. In the second-hop (FIUE to HIZUE (D2D link)),
595 there is reuse of radio resources which increases the interfer-
596 ence (explained in next paragraph). Hence, the cost can be ex-
597 pressed as given in Eq. (24), when the downlink scheduler at
598 Femto does not have excess resources.

Radio Resource Cost

$$= \sum_{i=1}^N \text{No of RBs allocated to FIUE}_i \text{ by Femto.} \quad (24)$$

599 Where N is the number of FIUEs participating as D2D based re-
600 lays for Femto to HIZUE communication.

- 601 2. **Interference:** In the first-hop there is no new interference source
602 introduced to the traditional system, whereas in the second-
603 hop (due to reuse of Femto RBs by D2D links) there is addi-
604 tional interference for the IUEs present in the system. This
605 could degrade SINR of IUEs and this reduction in SINR is the
606 additional cost incurred in the proposed system.
- 607 3. **Energy consumption:** In our work, the transmission power of
608 the Femto (first-hop communication) is kept as P_{max}^f (0.1 W)
609 to study the system performance in the worst case scenario. In
610 second-hop communication, the power consumed for the trans-
611 mission from FIUE to HIZUE, which varies based on distance be-
612 tween HIZUE and FIUE, is the cost to the system.

563 5. Performance results 613

614 The system model described in Section 4 has been simulated
615 using MATLAB. The simulation parameters are given in Table 5. We

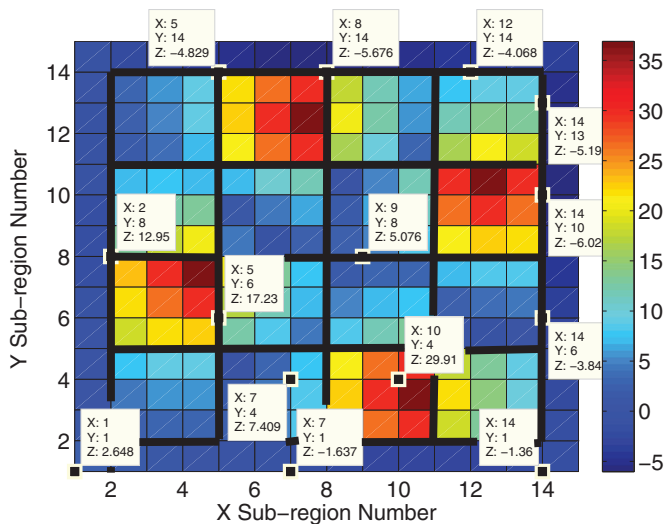


Fig. 6. REM plot of sub-regions inside building after placing Femtos by using MinNF. (For interpretation of the references to colour in the text, the reader is referred to the web version of this article.)

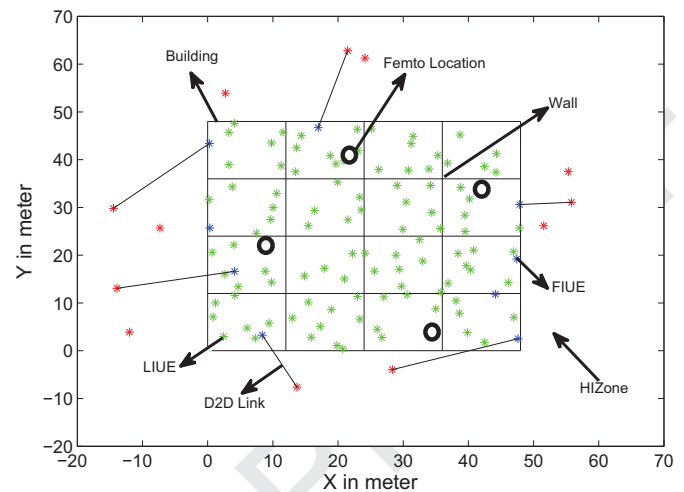


Fig. 7. hDPRA D2D links in instance #1. (For interpretation of the references to colour in the text, the reader is referred to the web version of this article.)

considered a single-floor building with a single MBS placed at a distance of 350 m from the south west side of the building. Further, we considered the scenario where all Femtos and MBS are configured to use the same 5 MHz channel (i.e., 25 RBs). Femtos are allowed to be attached only to the ceiling of the building and we did not consider the user mobility in our simulation experiments as we focused only on indoor scenarios. We show the performance of the LTE HetNet system in the worst case scenario where all RBs of all Femtos are in use in every TTI. Also we assume that channel state information of links between FIUEs and HI-Zones is available at the F-GW/SON for the fine tuning of D2D link transmission power. For the performance evaluation, we generate different topologies by varying number of UEs (i.e., IUEs and HIZUEs) and their positions in such a way that in each of the topologies that we considered there always exist one or more FIUEs for forming D2D links for each of the HIZUEs.

5.1. MinNF model: performance results

The four Femtos with their optimal coordinates are obtained by solving MinNF MILP problem with GAMS CPLEX solver [43]. The GAMS CPLEX solver is a high-level modeling system for optimization and utilizes branch and bound framework for solving MILP based optimization problems. This MILP optimizer has the capability to solve large and numerically difficult MILP models with features including settable priorities on integer variables, choice of different branching, and node selection strategies. The Femtos are placed in dark brown regions inside the building at sub-regions I_{30} , I_{71} , I_{98} , I_{129} (refer Fig. 5 for numbering of sub-regions) as shown in Fig. 6. All the Femtos transmit at their peak power (0.1 W). Fig. 6 also shows SINR distribution for inner and outer sub-regions. For example, UEs in the sub-region I_{98} get SINR of 29.9 dB as the Femto (F3) is very close to it. Similarly, the sub-regions I_6 , I_{29} , I_{79} , and I_{51} inside the building have relatively good SINR values 12.9, 17.2, 5.0, 7.4 dB, respectively. But if we consider Macro only scenario, where there are no Femtos inside the building like in Fig. 1, the sub-regions I_6 , I_{29} , I_{79} , and I_{51} inside the building have relatively less SNR values of -8.2 , -8.3 , -9.2 , -8.3 dB, respectively due to poor indoor signal strength.

Due to addition of Femtos, the UEs present inside the building get improved SINR up to 35 dB (refer Fig. 6). But in this case, the outer sub-regions (e.g., O_{48}), get SINR as low as -6.0 dB. This is

a consequence of Femtos being closer to the corners of the building and hence there being a high power leakage (interference) in HI-Zone.

5.2. D2D based relays: performance results

In this section, we compare the performance of proposed D2D MILP model and D2D heuristic algorithm with the following three different schemes.

- *Macro only:* No Femtos are placed inside the building. No HI-Zone exists around the building, but the MBS has to serve even IUEs with poor signal quality.
- *Full Power Femto:* Femtos are optimally placed inside the building by MinNF method, but Femtos are configured to emit at their full transmission power. In this scheme, HI-Zone exists around the building and therefore affects performance of HIZUEs.
- *Optimal Femto Power (OptFP):* Femtos are optimally placed inside the building by MinNF method, but transmission power of all the Femtos are reduced by OptFP method to decrease the interference to HIZUEs. Since such reduction at all the Femtos is not needed, this scheme affects performance of IUEs.

5.2.1. D2D heuristic algorithm: performance results

In this section, we show the formation of efficient D2D links and SINR CDF of UEs. Also, we studied the effect of $SINR_{th}$ on SINR of IUEs and effect of IUE density on FIUEs transmission power. Finally, we have shown the average performance of D2D heuristic algorithm by considering 500 different combinations of IUEs and HIZUEs location.

5.2.1.1. Formation of D2D links and their effects on SINR of UEs. In this section, we describe the hDPRA which efficiently chooses the potential D2D based relay pairs and allocates radio resources to them. Then we discuss about the performance of hDPA for power control of D2D links.

(a) hDPRA results:

The optimal Femto locations given by the MinNF model are shown as the circled regions in Fig. 7. The red, green and blue marked locations are the positions of the deployed HIZUEs, LIUEs and FIUEs, respectively in this topology # 1. These UEs locations at a particular instance (TTI) along with other parameters are given as input to the proposed heuristic algorithm. In Fig. 7, D2D connectivity diagram shows the number of D2D links in the instance #1. On

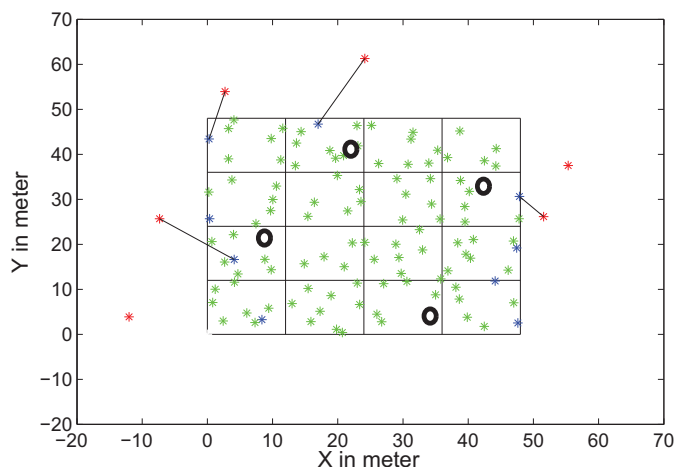


Fig. 8. hDPRA D2D links in instance #2.

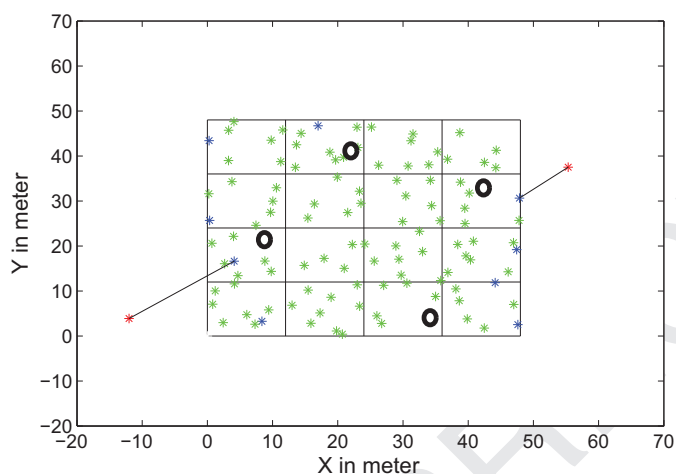
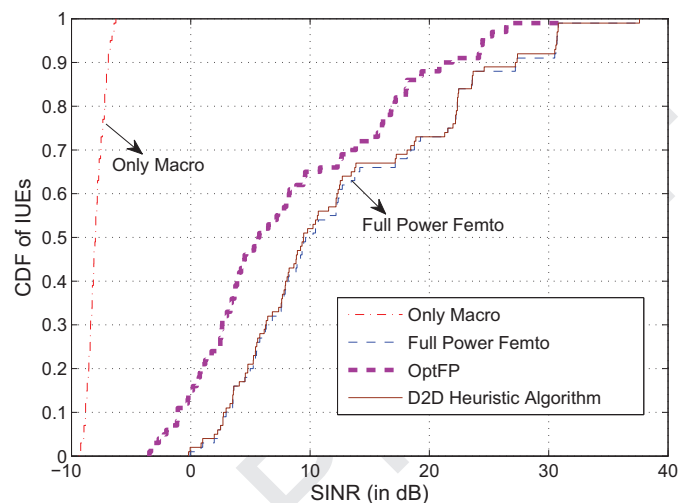
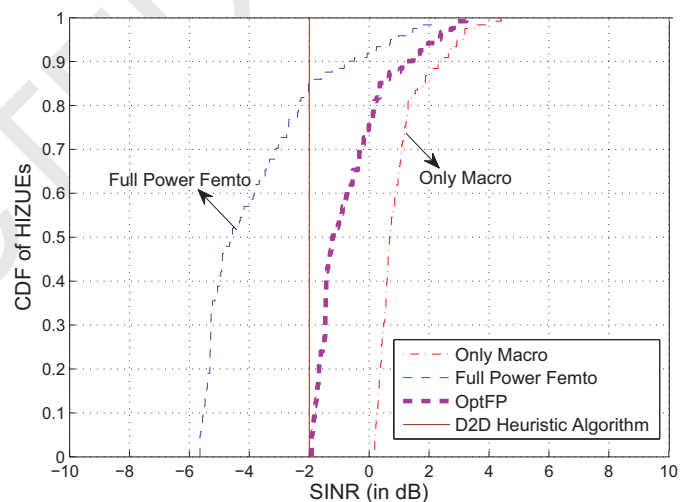


Fig. 9. hDPRA D2D links in instance #3.

696 one hand, there are relatively less number of *HIZUEs* at the south
 697 side of the building, but on the other hand, at the east, west and
 698 north sides of the building, there are some *HIZUEs* not served by
 699 *FIUE* in a particular TTI. It has to be kept in mind that a *HIZUE*
 700 can connect to only one *FIUE* in a given TTI as shown in all sides
 701 of the building. The reason for the other *HIZUE* to not connect is
 702 that even when there are certain free RBs that are not used by
 703 other D2D links, there is a possible interference between the *LI-*
 704 *UEs* or the possibility of guaranteeing an SINR threshold only by
 705 increasing the transmission power for D2D links above the 3GPP
 706 standards [22,44]. Hence, the *HIZUE* that does not get paired in
 707 the given TTI, get paired in subsequent TTIs. Figs. 8 and 9 show the
 708 pending D2D link connections to be made in subsequent instances.
 709 The output from hDPRA is given as the input to GAMS CPLEX
 710 solver [43] through an interface between MATLAB and GAMS to
 711 solve the hDPA LP model. Solving the hDPA model yields the trans-
 712 mission power for the D2D links.

713 (b) hDPA results:

714 Figs. 10 and 11 show the SINR CDF of *HIZUEs* and *IUEs*, respec-
 715 tively. In *Only Macro* scheme (shown by red curve) the *HIZUEs* re-
 716 ceive good SINR values but the *IUEs* receive very less SINR values,
 717 less than -5 dB which is due to the signal degradation caused by
 718 the walls. In our evaluation, we considered the worst case scenario
 719 where the *Full Power Femto* scheme (shown by blue curve) has in-
 720 creased SINR for the *IUEs* but at the cost of the SINR of *HIZUEs*. To
 721 overcome this issue, Femtos are made to transmit at lower power

Fig. 10. SINR CDF of *IUEs* using heuristic algorithm. (For interpretation of the references to colour in the text, the reader is referred to the web version of this article.)Fig. 11. SINR CDF of *HIZUEs* using heuristic algorithm. (For interpretation of the references to colour in the text, the reader is referred to the web version of this article.)

722 in the *OptFP* [1] i.e., *OptFP* scheme (shown by purple curve) thus
 723 alleviating the interference issues of *HIZUEs*, although this declines
 724 the SINR value of *IUEs*. However in *D2D heuristic algorithm* scheme
 725 (shown by brown curve) *HIZUEs* receive good SINR values and the
 726 *IUEs* also receive SINR values close to that of *Full Power Femto*
 727 scheme (worst case scenario). The straight line in Fig. 11 repre-
 728 sents the SINR value of *HIZUEs* using *D2D heuristic algorithm* main-
 729 tained at -2 dB constraint (to ensure basic voice call communi-
 730 cation for all suffering *HIZUEs*) of outdoor (*HIZone*) region. This is
 731 achieved by minimizing total transmit power of *FIUEs*, and thus the
 732 minimum power required to guarantee $SINR_{th}$ ensures that all the
 733 *HIZUEs* achieve $SINR_{th}$. The small deviation in the *IUEs* SINR values
 734 is because of the interference caused by the D2D pairs. The overall
 735 degradation in SINR for *IUEs* is 2% in the *D2D heuristic algorithm*
 736 as compared to the *Full Power Femto* scheme. But in comparison
 737 to the *OptFP* [1] scheme the SINR of *IUEs* improves by 39% for the
 738 *D2D heuristic algorithm*. Thus *D2D heuristic algorithm* is able to pro-
 739 vide a good signal strength to the *HIZUEs* without affecting the *IUE*
 740 performance.

741 5.2.1.2. Effect of $SINR_{th}$ on SINR of *IUEs*. We studied the variation
 742 in SINR of *IUEs* by varying $SINR_{th}$ values. We also measured the

Table 4
Simulation parameters.

Parameter	Value
Building dimensions	48 m × 48 m × 3 m
Number of rooms	16
Room dimensions	12 m × 12 m × 3 m
Number of inner sub-regions	144
Number of outer sub-regions	52
Inner sub-region dimension	4 m × 4 m × 3 m
$SINR_{th}$ for IUEs (MinNF method)	0 dB
Number of floor	One
Floor and wall loss	10 and 8 dB
Macro transmit power (P_{macro})	46 dBm (39.8 W)
Femto transmit power (P_{max}^f)	20 dBm (0.1 W)
Macro BS height	30 m
D2D Max transmit power (P_{max}^d)	20 dBm (0.1 W)
Number of IUEs	109
HIZUE $SINR_{th}$	-2 dB
α (FIUE D2D links limit)	1
β (HIZUE D2D links limit)	1
$\bar{\gamma}$ (W2L Threshold)	5

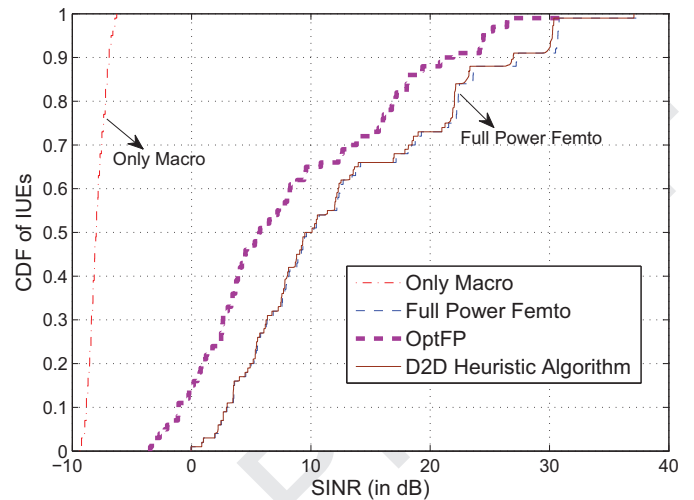


Fig. 12. Average SINR CDF of IUEs for various schemes in 500 topologies.

743 variation in average D2D transmission power for topology # 1. As
 744 shown in Table 4, the average transmit power of D2D links in-
 745 creases gradually with increasing $SINR_{th}$. This increases the inter-
 746 ference to the IUEs and hence causes a fall in average IUE SINR
 747 with increase in $SINR_{th}$ of HIZUEs. We note that even with changes
 748 in $SINR_{th}$ the degradation of IUEs SINR is not very significant. This
 749 validates the efficiency of our D2D heuristic algorithm.

750 **5.2.1.3. Effect of IUE density on FIUEs transmission power.** In our
 751 work, we studied the variation in D2D transmission power. Here
 752 we consider topology # 1 as above but vary the number of FIUEs
 753 for a fixed HIZUE location (shown in Fig. 7). Initially, the total num-
 754 ber of IUEs is 110 (i.e., LIUEs = 100 (constant) and FIUEs = 10) and
 755 we gradually increase only the FIUEs count to 15, 20, 25, 30 and
 756 35. Table 6 shows that as the number of FIUEs increases, the average
 757 transmit power of FIUEs decreases. This is due to the increased
 758 possibility of forming shorter D2D based relay links with increasing
 759 FIUE density levels. Once the FIUEs density level is very high, the
 760 transmission power of the FIUEs will get saturated due to marginal
 761 decrease in D2D relay link distance.

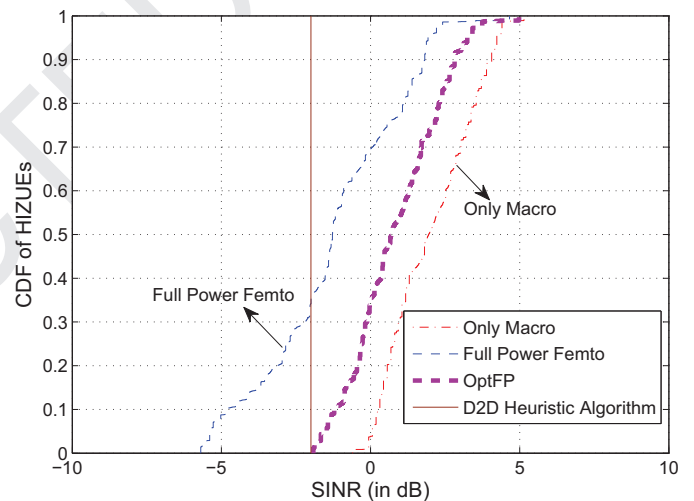


Fig. 13. Average SINR CDF of HIZUEs for various schemes in 500 topologies.

762 **5.2.1.4. Average performance of D2D heuristic algorithm.** In order to
 763 obtain average performance of proposed D2D heuristic algorithm,
 764 we have evaluated its performance for 500 different topologies by
 765 varying the number of IUEs in the range of 110 to 135 and HIZUEs
 766 in the range of 1 to 30 and measured the SINR of IUEs and HIZUEs.
 767 Fig. 12 shows SINR CDF of IUEs over various scenarios for differ-
 768 ent schemes. When compared to the Optimal Femto Power scheme,
 769 D2D heuristic algorithm improves the SINR of IUEs by 40% as shown
 770 in Fig. 12. However, the degradation in SINR of IUEs is only 1.6%
 771 when compared to the Full Power Femto scheme. Similarly, Fig. 13
 772 shows average CDFs of HIZUEs over various scenarios for different
 773 schemes. If we observe Fig. 13, the minimum $SINR_{th} = -2$ dB is
 774 maintained for all HIZUEs in the HIZone.

775 **5.2.2. D2D MILP model: performance analysis**

776 In the proposed D2D heuristic algorithm, we cannot set the
 777 number of D2D links in each TTI. To make a fair comparison with

Table 6
Number of FIUEs vs. average D2D transmission power.

S.no.	No. of FIUEs	Average D2D transmission power (W)
1	10	0.061
2	15	0.054
3	20	0.051
4	25	0.043
5	30	0.042
6	35	0.041

the D2D MILP model, we have given the number of D2D links ob- 778
 tained from the D2D heuristic algorithm in each instance as an 779
 input for the D2D MILP model. For example, for the instance #1 780
 shown in Fig. 7 the number of D2D links given by the heuristic al- 781
 gorithm is six. Hence in the D2D MILP model the number of D2D 782

Table 5
 $SINR_{th}$ vs. IUEs SINR.

Metric	$SINR_{th} = -3$ dB	$SINR_{th} = -2$ dB	$SINR_{th} = -1$ dB	$SINR_{th} = 0$ dB
Average transmission power of D2D links (W)	0.03	0.04	0.05	0.06
Average IUEs SINR (dB)	12.78	12.75	12.72	12.68

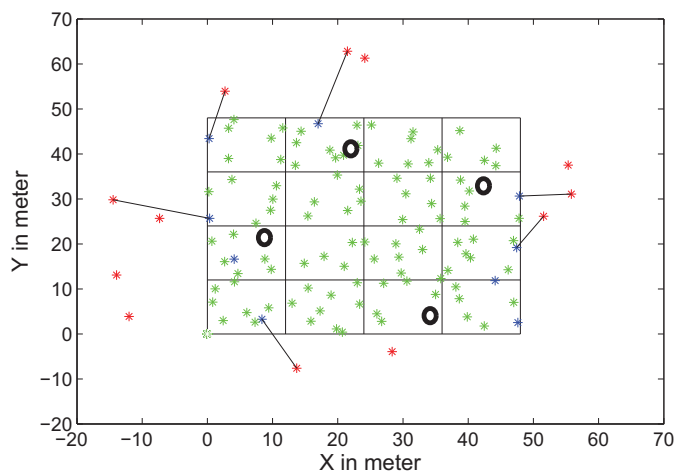


Fig. 14. MILP D2D links in instance #1.

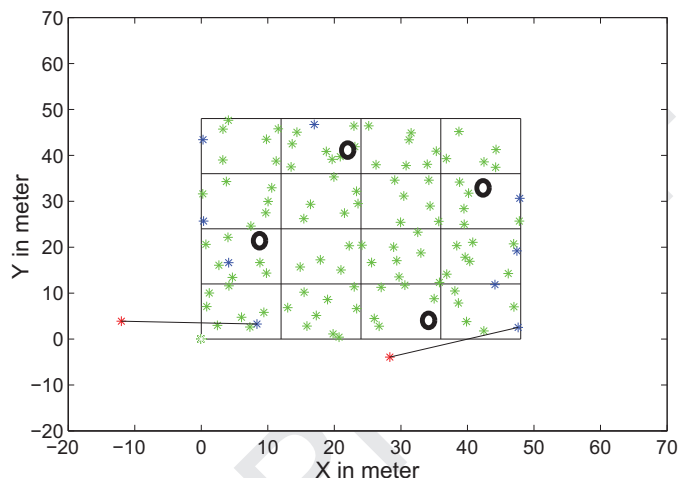


Fig. 16. MILP D2D links in instance #3.

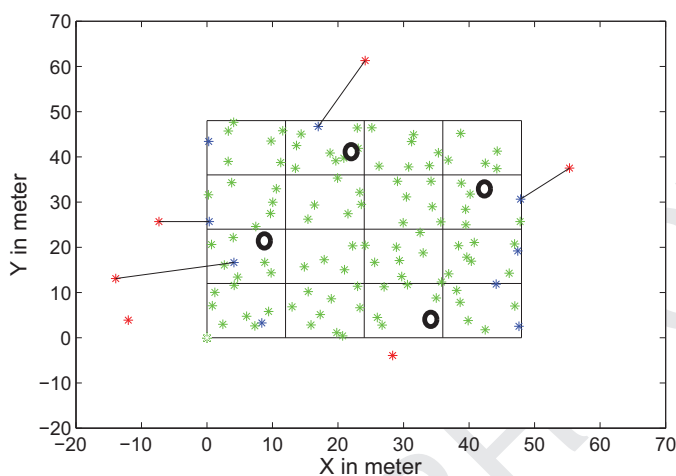


Fig. 15. MILP D2D links in instance #2.

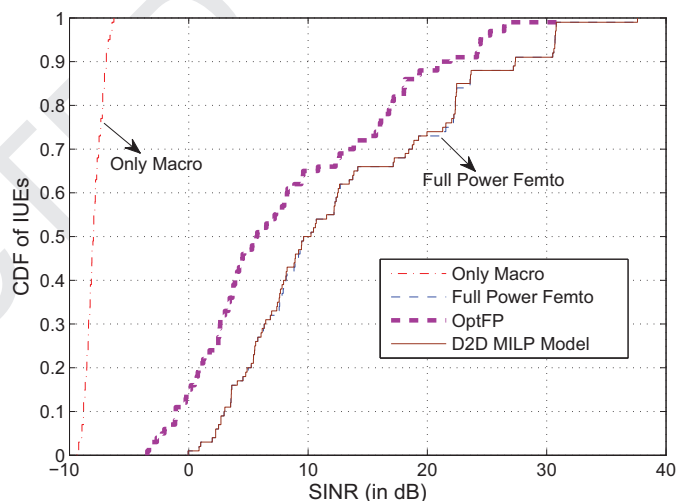


Fig. 17. SINR CDF of IUEs using MILP model.

783 links that have to be formed at the instance #1 is fixed to be six,
784 i.e., $\psi = 6$.

785 In Fig. 14, D2D connectivity diagram shows the number of D2D
786 links in the instance #1. As in the heuristic algorithm, there are
787 some HIZUEs which are not served by FIUEs in a particular TTI. The
788 pending HIZUEs served by FIUEs based on the D2D MILP model
789 are shown in Figs. 15 and 16. In the instance #1, the algorithm
790 mostly tries to form all D2D links with the closer HIZUEs to mini-
791 mize the total D2D transmission power. In the next TTI, it tries to
792 form the remaining D2D links with the farther HIZUEs. Hence the
793 FIUE needs to transmit high transmission power to maintain these
794 D2D links, which increases the possibility of interference between
795 LIUEs and HIZUEs. Fig. 17 shows the SINR CDF of IUEs. The advan-
796 tage of forming optimal D2D link is that D2D MILP model achieves
797 SINR close to that of Full Power Femto because the power value
798 is optimal. Similarly, the SINR CDF of HIZUEs in optimal approach
799 (D2D MILP) is also maintained $SINR_{th} = -2$ dB as in the heuris-
800 tic approach (Fig. 11). The SINR CDF of HIZUEs using MILP model
801 will be same as that of the heuristic algorithm (Fig. 11) because
802 the same $SINR_{th}$ is maintained in both D2D heuristic algorithm and
803 D2D MILP model. The overall degradation in SINR for IUEs is 0.5%
804 in the D2D MILP model compared to the Full Power Femto scheme.
805 On the other hand, when compared to OptFP [1] scheme the SINR
806 of IUEs improves by 52% in the D2D MILP model. Thus D2D MILP
807 model is able to provide lesser degradation in signal strength to

the IUEs than the D2D heuristic algorithm with the cost of more 808
809 running time (explained further in Section 5.3.2).

5.3. Comparison between D2D MILP model and D2D heuristic algorithm 810 811

To compare D2D MILP model and D2D heuristic algorithm, we 812
813 have taken the seven different topologies, where the HIZUE place-
814 ment and the number of HIZUEs vary as shown in Figs. 18–24.
815 Table 7 shows indices of outer sub-regions having HIZUEs in these
816 seven topologies.

5.3.1. SINR of IUEs 817

In MILP model, the average power transmitted by the D2D links 818
819 is lower than that in the heuristic algorithm. This helps to reduce
820 the interference to IUEs. Fig. 25 shows the average SINR achieved
821 by IUEs in different topologies. The average SINR achieved in the
822 heuristic algorithm is very close to that in the D2D MILP model.

5.3.2. Running time 823

Fig. 26 shows the average running times of D2D MILP model 824
825 and D2D heuristic algorithm for different topologies. These run
826 times are obtained on a workstation having the following configu-
827 ration: 12 GB RAM, eight Cores of 2.40 GHz each. We observe

Table 7
Topologies having varying distribution of HIZUEs in HIZone.

Topology	No. of HIZUEs	Indices of outer sub-regions having HIZone UEs
1	12	(O ₅ , O ₉ , O ₁₅ , O ₂₁ , O ₂₇ , O ₂₈ , O ₂₉ , O ₃₀ , O ₃₄ , O ₄₀ , O ₄₅ , O ₄₆)
2	15	(O ₃ , O ₅ , O ₁₀ , O ₁₂ , O ₁₄ , O ₁₈ , O ₂₃ , O ₂₅ , O ₃₀ , O ₃₂ , O ₄₁ , O ₄₄ , O ₄₅ , O ₄₆ , O ₄₈)
3	7	(O ₁ , O ₆ , O ₁₃ , O ₂₇ , O ₃₅ , O ₄₃ , O ₄₅)
4	10	(O ₁₇ , O ₂₃ , O ₂₉ , O ₆ , O ₉ , O ₁₃ , O ₂₂ , O ₂₆ , O ₃₅ , O ₄₆)
5	10	(O ₁ , O ₂₁ , O ₃₁ , O ₃₇ , O ₁₀ , O ₁₃ , O ₂₂ , O ₂₆ , O ₄₅ , O ₅)
6	13	(O ₁₅ , O ₂₁ , O ₃₁ , O ₄₁ , O ₄₅ , O ₈ , O ₁₀ , O ₁₄ , O ₂₀ , O ₂₂ , O ₂₆ , O ₅)
7	9	(O ₉ , O ₂₃ , O ₃₅ , O ₄₅ , O ₁₃ , O ₂₀ , O ₂₄ , O ₂₆ , O ₄)

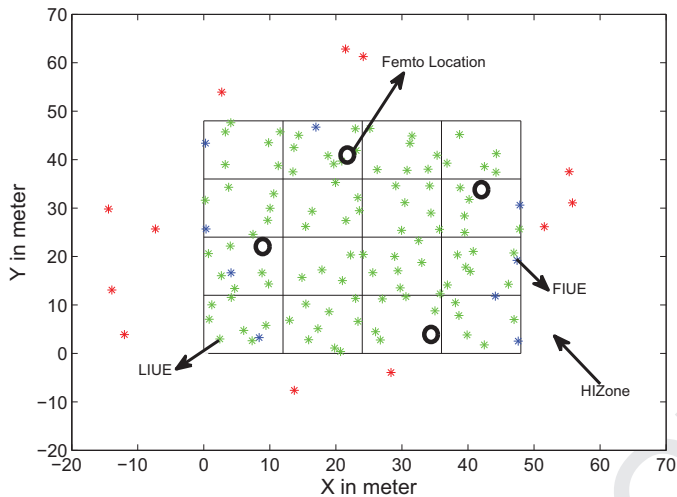


Fig. 18. UE distribution in Topology 1.

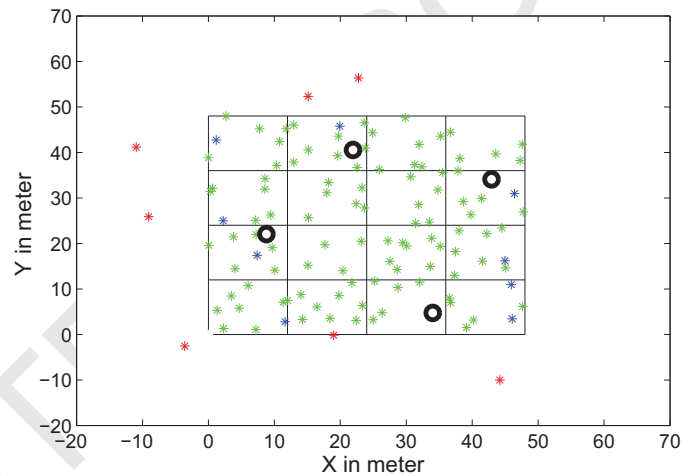


Fig. 20. UE distribution in Topology 3.

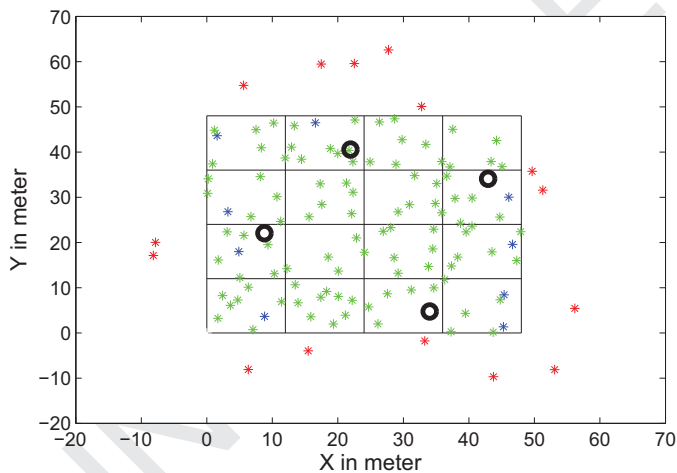


Fig. 19. UE distribution in Topology 2.

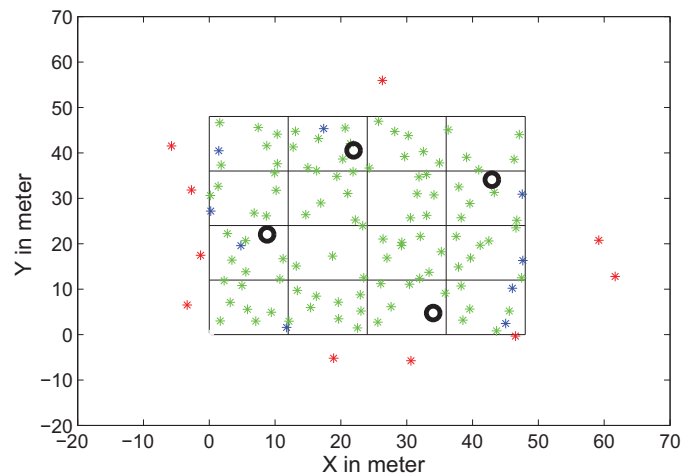


Fig. 21. UE distribution in Topology 4.

828 that the running time for *D2D heuristic algorithm* showed an average
 829 decrease of up to 87% when compared to *D2D MILP model* in
 830 different topologies of HIZUE placement. In each topology, depend-
 831 ing on the position of the HIZUEs, the running time of GAMS opti-
 832 mization solver changed. For example, when HIZUEs are very close
 833 to each other it demands efficient spectrum allocation and power
 834 control between FIUE and HIZUE in all instances without creating
 835 interference to IUEs. Therefore, on a few occasions many D2D links
 836 may not be possible within the HIZone at a particular TTI instance
 837 which indirectly increases the average running time. As we dis-
 838 cussed earlier in the system model, the D2D heuristic algorithm
 839 will be running at the F-GW/SON which will have abundant com-
 840 puting resources to handle the load of so many Femtos [45,46].

Therefore, the run time of *D2D heuristic algorithm* is only a few ms
 and usable in practical deployments of Femtos.

5.3.3. Energy consumption

Fig. 27 shows the average power transmitted by the D2D links
 for different topologies with the SINR_{th} = -2 dB. The average power
 transmitted by the D2D links (for example, it is 0.043 W and
 0.047 W in *D2D MILP model* and *D2D heuristic algorithm*, respec-
 tively) are lower than the maximum allowed D2D link power of
 0.1 W. We can clearly observe that the average transmission power
 of the D2D links in the heuristic algorithm is close to that in the
 MILP model and the difference between them is marginal.

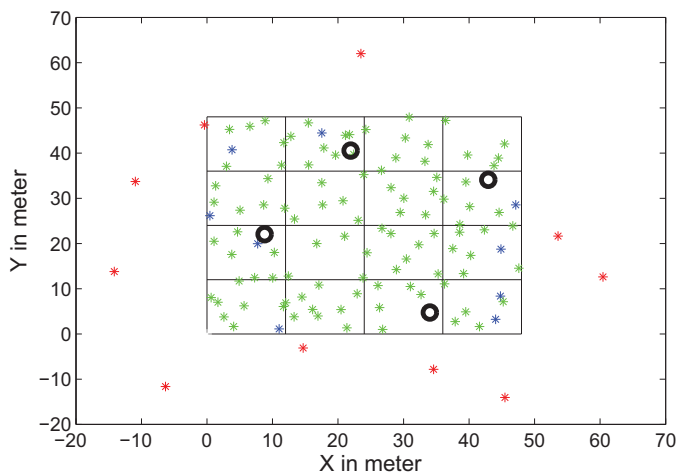


Fig. 22. UE distribution in Topology 5.

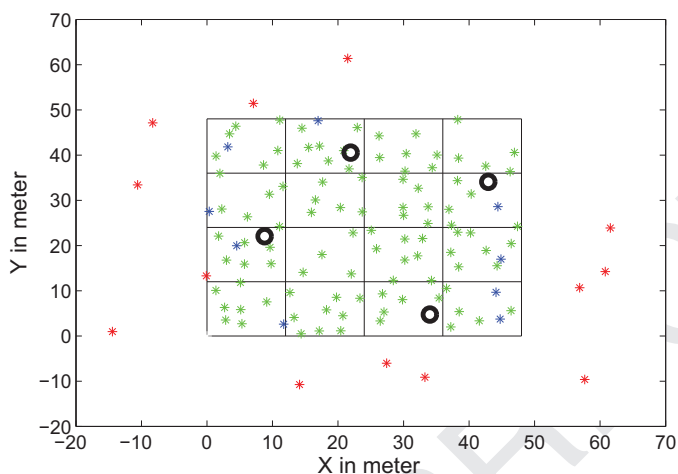


Fig. 23. UE distribution in Topology 6.

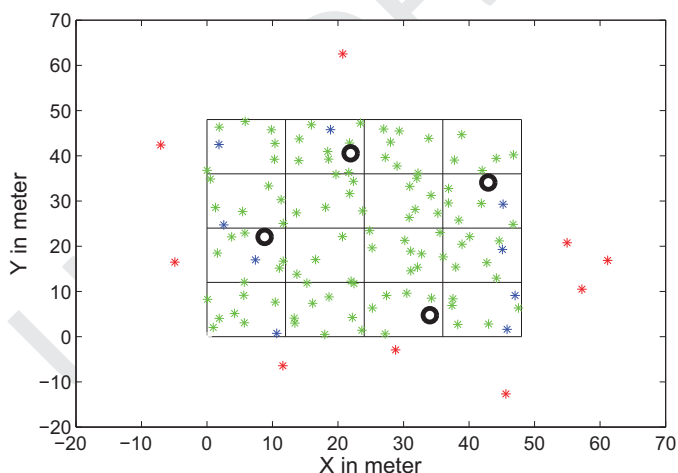


Fig. 24. UE distribution in Topology 7.

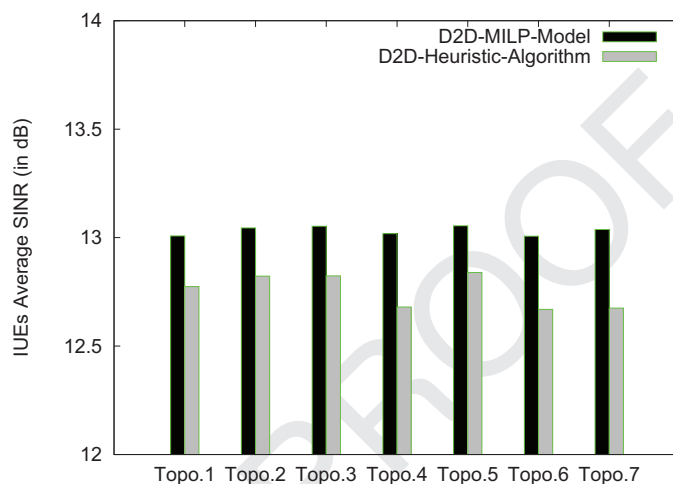


Fig. 25. Average SINR of IUEs.

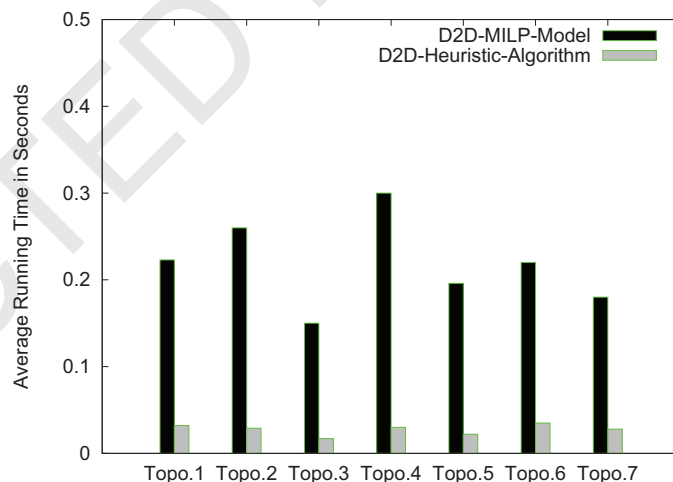


Fig. 26. Running time of D2D MILP and heuristic algorithm.

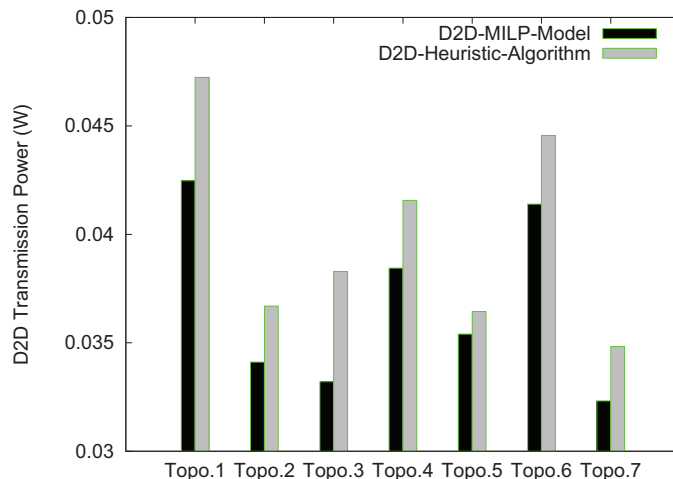


Fig. 27. D2D average transmission power.

5.4. Cost analysis

In our work we assumed that the downlink scheduling algorithm [47] (e.g., proportional fair or priority set scheduler) will allocate only one resource block to the selected Femto to FIUE links or FIUE to HIZUE links in every TTI. Using this, we have simulated 500 different possible combinations for IUEs and HIZUEs locations

and observed that an average of 5 D2D links are formed in a TTI. Hence, five resource blocks will be used for the first-hop i.e., Femto to FIUE link to get the data for HIZUEs. This means that these five resource blocks are the radio resource cost.

The D2D based relay links will reuse these five Femto RBs in the second-hop transmission (FIUE to HIZUE) [48–50]. The interference introduced in the system by these D2D based relay links leads

858
859
860
861
862
863
864

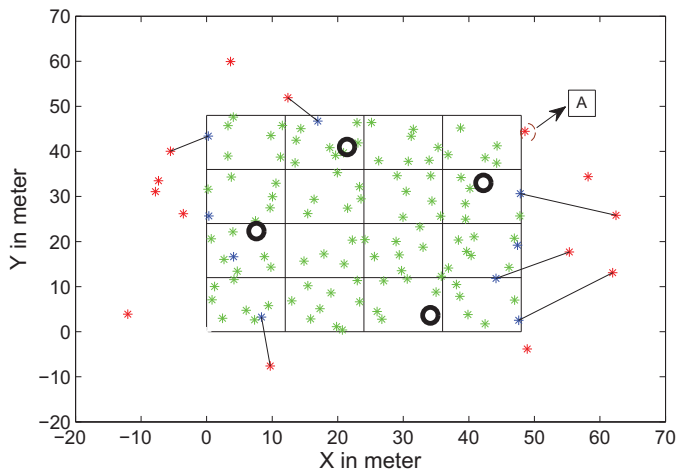


Fig. 28. hDPRA D2D links in instance #1.

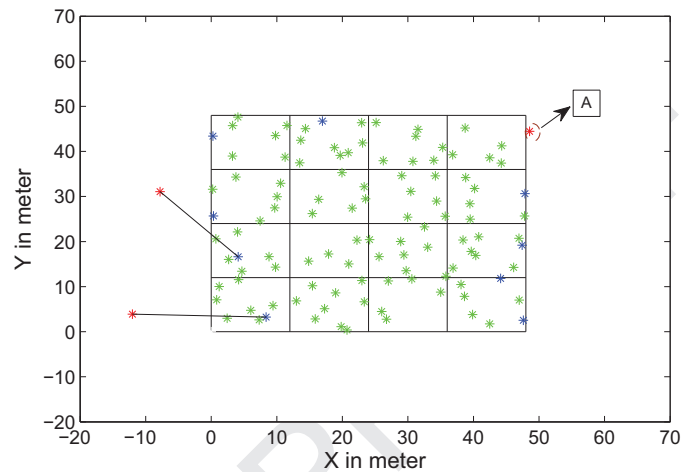


Fig. 30. hDPRA D2D links in instance #3.

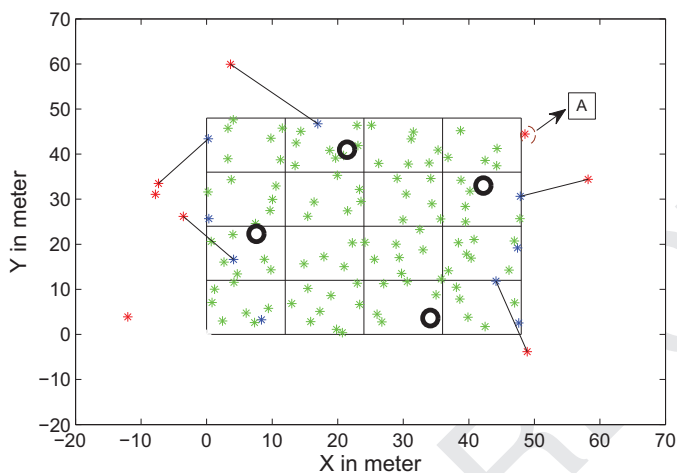


Fig. 29. hDPRA D2D links in instance #2.

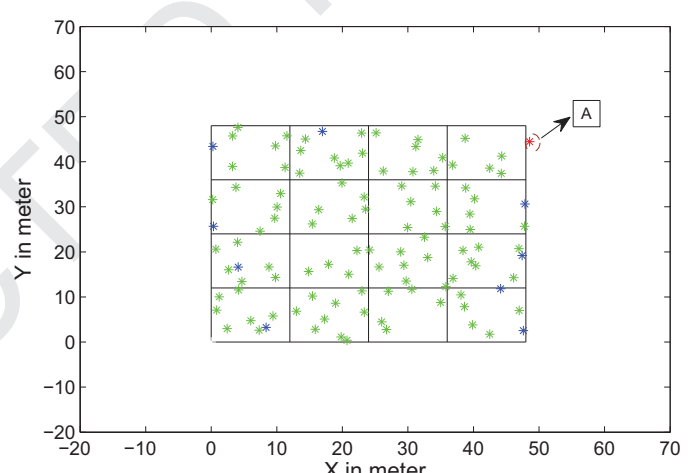


Fig. 31. hDPRA D2D links in instance #4.

865 to decrease in the SINR of IUEs by 1.6% (averaged over 500 scenarios).
 866 This is the cost of using the proposed system in terms of
 867 interference.

868 As shown in Fig. 27, the transmission power of the D2D links is
 869 adjusted in order to maintain the $SINR_{th}$ of -2 dB for HIZUEs. Be-
 870 cause of power adjustment, D2D links are able to reuse the same
 871 RBs and thereby improve the spectral efficiency of the HetNet system.
 872 Hence, the total energy consumption [51] in the two-hop
 873 communication is $0.1 W + D2D$ based relay transmission power.

874 5.5. JDHO performance analysis

875 Unlike the previous section, here we study the performance
 876 of JDHO algorithm by considering a topology where some of the
 877 HIZUEs could not able to make D2D links due to lack of FIUEs.
 878 As seen in Algorithm 2 (Step 6), these O' HIZUEs connect to the
 879 MBS for their D-plane communication. The remaining HIZUEs
 880 (i.e., $(O - O')$) form D2D links with FIUEs by using proposed D2D
 881 heuristic algorithm. Consider the topology shown in Fig. 28, where
 882 one can see that there are no FIUEs in the vicinity of HIZUE A.
 883 D2D heuristic algorithm which is running at F-GW cannot able to
 884 form any D2D link for serving the HIZUE A. In order to reduce
 885 interference at this HIZUE in the HIZone, JDHO algorithm controls
 886 the transmit power of the Femto which is serving the parts of the
 887 building closest to this region. By doing so, the HIZUE A can main-
 888 tain a minimum $SINR_{th}$ in HIZone. Figs. 29–31 show the pending
 889 D2D links established in the subsequent instances. When com-

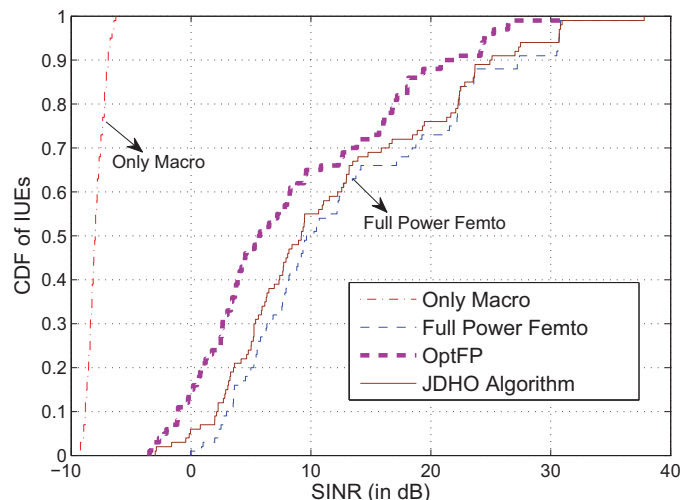


Fig. 32. SINR CDF of IUEs using JDHO algorithm.

890 pared to Full Power Femto scheme where the degradation of IUEs
 891 SINR is found to be 2% as obtained in the previous case (shown
 892 in Fig. 10), in the current JDHO algorithm scenario as shown in
 893 Fig. 32 the degradation of IUEs SINR was found to be 9%. This is
 894 because, to maintain the communication (D-Plane) for HIZUE A
 895 from MBS, the corresponding/particular Femto has to optimally

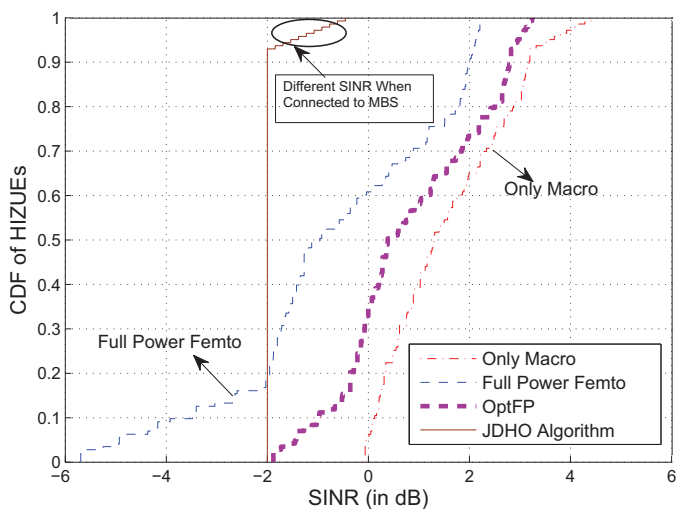


Fig. 33. SINR CDF of HIZUEs using JDHO algorithm.

896 decrease its transmission power further to reduce the SINR of IUEs.
 897 Fig. 33 shows that HIZUEs maintained $SINR_{th}$ when JDHO algorithm
 898 is used. In previous scenario (shown in Fig. 11) we maintained a
 899 constant $SINR_{th}$ to all HIZUEs. But in the present scenario, in JDHO
 900 algorithm by using the OptFP model, the $SINR_{th}$ for HIZUE A is
 901 maintained at more than -2 dB (as shown in circle region).

902 6. Conclusions and future work

903 In this paper, we showed that D2D technology when adopted
 904 to LTE HetNets increases the spectrum efficiency by guaranteeing
 905 good $SINR_{th}$ for all the users even when the Femtos are trans-
 906 mitting at their full power. By introducing Femtos, a fair distribu-
 907 tion for both IUEs and HIZUEs with minimal interference can be
 908 observed. Additionally, an increase in SINR values of IUEs by 40%
 909 compared to the OptFP [1] scheme was noted in D2D heuristic al-
 910 gorithm. On the other hand, the decrease in the SINR of IUEs com-
 911 pared to the Full Power Femto scheme is only 1.6%. We also ob-
 912 served that the average running time of the proposed D2D heuristic
 913 algorithm was 87% lesser when compared to D2D MILP model.

914 Future work includes design of an efficient scheduling algo-
 915 rithm that considers fair allocation of radio resources for both
 916 IUEs and HIZUEs and also study the additional signaling overhead
 917 caused by the D2D links in the proposed system. Optimization of
 918 the size of HIZone based on the D2D standards (i.e., maximum D2D
 919 link distance and transmit power) is also a future task.

920 Acknowledgment

921 This work was supported by the Deity, Govt of India (grant no.
 922 13(6)/2010CC&BT).

923 Appendix A

924 Running time complexity

925 The proposed D2D MILP model takes more computation time.
 926 To reduce the running time complexity, we have proposed a two-
 927 step D2D heuristic algorithm. The running time complexity for hD-
 928 PRA (step 1 of D2D heuristic algorithm) is shown below,

929 The time taken to compute maximum value in the γ matrix is
 930 $O(f * o * k)$

931 The running time for the while loop is $O(f * o * k)$

932 The total running time is $O(f^2 * o^2 * k^2)$

933 Since the step 2 of D2D heuristic algorithm (hDPA, an LP model)
 934 has a polynomial running time algorithm [52], our proposed D2D
 935 heuristic algorithm runs in polynomial time.

References

- [1] V. Sathya, A. Ramamurthy, B.R. Tamma, On placement and dynamic power control of femtocells in LTE HetNets, in: 2014 IEEE Global Communications Conference (GLOBECOM), 2014, pp. 4394–4399. 937
- [2] Enterprise Multi-femtocell Deployment Guidelines, Qualcomm Inc., 2011. 938
- [3] CISCO VNI Data, <http://www.cisco.com/c/en/us/solutions/service-provider/visual-networking-index-vni/index.html>. 939
- [4] Views on Rel-12 and onwards for LTE and UMTs, Future Radio in 3GPP, Huawei Technologies, 2012. 940
- [5] V. Chandrasekhar, J.G. Andrews, A. Gatherer, Femtocell networks: a survey, IEEE Commun. Mag. 46 (9) (2008) 59–67. 941
- [6] I.E. Ahmed, B.R. Qazi, J.M. Elmighani, Base stations locations optimisation in an airport environment using genetic algorithms, in: 2012 Eighth International Wireless Communications and Mobile Computing Conference (IWCMC), IEEE, 2012, pp. 24–29. 942
- [7] W. Guo, S. Wang, Interference-aware self-deploying femto-cell, IEEE Wireless Commun. Lett. 1 (6, December) (2012). 943
- [8] W. Guo, S. Wang, X. Chu, J. Zhang, J. Chen, H. Song, Automated small-cell deployment for heterogeneous cellular networks, IEEE Commun. Mag. 51 (5) (2013) 46–53. 944
- [9] J. Liu, Q. Chen, H.D. Sherali, Algorithm design for femtocell base station placement in commercial building environments, in: INFOCOM, IEEE, 2012, pp. 2951–2955. 945
- [10] M. Tahalani, V. Sathya, A. Ramamurthy, U. Suhas, M.K. Giluka, B.R. Tamma, Optimal placement of femto base stations in enterprise femtocell networks, in: 2014 IEEE International Conference on Advanced Networks and Telecommunications Systems (ANTS), IEEE, 2014, pp. 1–6. 946
- [11] Y. Lin, W. Yu, Y. Lohan, Optimization of wireless access point placement in realistic urban heterogeneous networks, in: 2012 IEEE GLOBECOM, IEEE, 2012, pp. 4963–4968. 947
- [12] K. Han, Y. Choi, D. Kim, M. Na, S. Choi, K. Han, Optimization of femtocell network configuration under interference constraints, in: WiOPT 2009, IEEE, 2009. 948
- [13] V. Sathya, A. Ramamurthy, B. Tamma, Joint placement and power control of LTE femto base stations in enterprise environments, in: 2015 International Conference on Computing, Networking and Communications (ICNC), 2015, pp. 1029–1033. 949
- [14] H. Ishii, Y. Kishiyama, H. Takahashi, A novel architecture for LTE-b: C-plane/u-plane split and phantom cell concept, in: 2012 IEEE Globecom Workshops (GC Wkshps), IEEE, 2012, pp. 624–630. 950
- [15] H. Lokhandwala, V. Sathya, B.R. Tamma, Phantom cell realization in LTE and its performance analysis, in: 2014 IEEE International Conference on Advanced Networks and Telecommunications Systems (ANTS), IEEE, 2014, pp. 1–6. 951
- [16] 3GPP Releases, <http://www.3gpp.org/releases>. 952
- [17] L. Wei, R.Q. Hu, Y. Qian, G. Wu, Enable device-to-device communications underlying cellular networks: challenges and research aspects, IEEE Commun. Mag. 52 (6) (2014) 90–96. 953
- [18] P. Phunchongham, E. Hossain, D.I. Kim, Resource allocation for device-to-device communications underlying LTE-advanced networks, IEEE Wireless Commun. 20 (4) (2013). 954
- [19] A. Asadi, Q. Wang, V. Mancuso, A survey on device-to-device communication in cellular networks, IEEE Commun. Surv. Tutor. 16 (4) (2014) 1801–1819. 955
- [20] L. Lei, Z. Zhong, C. Lin, X. Shen, Operator controlled device-to-device communications in LTE-advanced networks, IEEE Wireless Commun. 19 (3) (2012) 96. 956
- [21] B. Raghothaman, E. Deng, R. Pragada, G. Sternberg, T. Deng, K. Vanganuru, Architecture and protocols for LTE-based device to device communication, in: ICNC 2013, IEEE, 2013, pp. 895–899. 957
- [22] M. Zulhasnine, C. Huang, A. Srinivasan, Efficient resource allocation for device-to-device communication underlying LTE network, in: WiMob 2010, IEEE, 2010, pp. 368–375. 958
- [23] F. Malandrino, C. Casetti, C.-F. Chiasserini, Z. Limani, Fast resource scheduling in HetNets with D2D support, arXiv:1311.6837 (2013). 959
- [24] H. Ishii, X. Cheng, S. Mukherjee, B. Yu, An LTE offload solution using small cells with D2D links, in: IEEE ICC 2013, IEEE, 2013, pp. 1155–1160. 960
- [25] T. Bansal, K. Sundaresan, S. Rangarajan, P. Sinha, R2d2: embracing device-to-device communication in next generation cellular networks, Cell 50 (3) (2014) 3–9. 961
- [26] K. E. Sambo, S. Muhammad, Expanding cellular coverage via cell-edge deployment in heterogeneous networks: spectral efficiency and backhaul power consumption perspectives, IEEE Commun. Mag. 52 (6) (2014) 140–149. 962
- [27] C. Gao, X. Sheng, J. Tang, W. Zhang, S. Zou, M. Guizani, Joint mode selection, channel allocation and power assignment for green device-to-device communications, in: IEEE ICC 2014, IEEE, 2014, pp. 178–183. 963
- [28] H. Nishiyama, M. Ito, N. Kato, Relay-by-smartphone: realizing multihop device-to-device communications, IEEE Commun. Mag. 52 (4) (2014) 56–65. 964
- [29] M. Alam, D. Yang, J. Rodriguez, R. Abd-Alhameed, Secure device-to-device communication in LTE-a, IEEE Commun. Mag. 52 (4) (2014) 66–73. 965
- [30] N. Bhushan, J. Li, D. Malladi, R. Gilmore, D. Brenner, A. Damnjanovic, R. Sukhvasi, C. Patel, S. Geirhofer, Network densification: the dominant theme for wireless evolution into 5 g, IEEE Commun. Mag. 52 (2) (2014) 82–89. 966
- [31] A. Orsino, L. Militano, G. Araniti, A. Molinaro, A. Iera, Efficient data uploading supported by D2D communications in LTE-a systems, arXiv:1503.09076 (2015). 967

- 1017 [32] G. Rigazzi, F. Chiti, R. Fantacci, C. Carlini, Multi-hop D2D networking and resource management scheme for M2M communications over LTE-a systems, in: 2014 International Wireless Communications and Mobile Computing Conference (IWCMC), IEEE, 2014, pp. 973–978.
- 1018
- 1019
- 1020
- 1021 [33] J.M.B. da Silva, G. Fodor, T.F. Maciel, Performance analysis of network-assisted two-hop D2D communications, in: 2014 Globecom Workshops (GC Wkshps), IEEE, 2014, pp. 1050–1056.
- 1022
- 1023
- 1024 [34] S. Doumiati, H. Artail, D.M. Gutierrez-Estevez, A framework for LTE-a proximity-based device-to-device service registration and discovery, Proc. Comput. Sci. 34 (2014) 87–94.
- 1025
- 1026
- 1027 [35] G. Fodor, E. Dahlman, G. Mildh, S. Parkvall, N. Reidler, G. Miklós, Z. Turányi, Design aspects of network assisted device-to-device communications, IEEE Commun. Mag. 50 (3) (2012) 170–177.
- 1028
- 1029
- 1030 [36] Sounding Reference Signal, http://www.sharetechnote.com/html/Handbook_LTE_SRS.html.
- 1031
- 1032 [37] K. Lee, W. Kang, H.-J. Choi, A practical channel estimation and feedback method for device-to-device communication in 3GPP LTE system, in: Proceedings of the Eighth International Conference on Ubiquitous Information Management and Communication, ACM, 2014, p. 17.
- 1033
- 1034
- 1035
- 1036 [38] J. Jang, H. Cho, Y. Kwon, H. Lee, Communication method between terminals, and terminal, 2013, EP Patent App. EP20,110,759,661.
- 1037
- 1038 [39] M.J. Yang, S.Y. Lim, H.J. Park, N.H. Park, Solving the data overload: device-to-device bearer control architecture for cellular data offloading, IEEE Vehic. Technol. Mag. 8 (1) (2013) 31–39.
- 1039
- 1040
- 1041 [40] 3GPP, 3GPP TSGSA: Feasibility Study for Proximity Services (ProSe) (Release 12), 3GPP, Technical Report TR 22.803, Aug 2013.
- 1042
- 1043 [41] X. Lin, J.G. Andrews, A. Ghosh, R. Ratasuk, An overview of 3GPP device-to-device proximity services, IEEE Commun. Mag. 52 (4) (2014) 40–48.
- 1044
- 1045 [42] A. Hameed, A. Oudah, Interference in wireless networks: causes, analyses and practical mitigating techniques, Mod. Appl. Sci. 8 (5) (2014) p56.
- 1046
- 1047 [43] GAMS, <http://www.gams.com/>.
- 1048 [44] 3GPP, 3GPP: LTE; E-UTRA; UE Radio Transmission and Reception, 3GPP, Tech. Rep. TR 25.101, March 2015.
- 1049
- 1050 [45] White Paper—Radsys: SCTP Fast Path Optimization for 3G/LTE Networks.
- 1051 [46] Continuous Computing: Trillium Femtocell Gateway,
- 1052 [47] F. Capozzi, G. Piro, L.A. Grieco, G. Boggia, P. Camarda, Downlink packet scheduling in LTE cellular networks: key design issues and a survey, IEEE Commun. Surv. Tutor. 15 (2) (2013) 678–700.
- 1053
- 1054 [48] T.D. Hoang, L.B. Le, T. Le-Ngoc, Resource allocation for D2D communications under proportional fairness, in: 2014 IEEE Global Communications Conference (GLOBECOM), IEEE, 2014, pp. 1259–1264.
- 1055
- 1056 [49] R.L. Batista, J.M.B. da Silva, T.F. Maciel, F.R.P. Cavalcanti, et al., What happens with a proportional fair cellular scheduling when D2D communications underlay a cellular network? in: 2014 IEEE Wireless Communications and Networking Conference Workshops (WCNCW), IEEE, 2014, pp. 260–265.
- 1057
- 1058 [50] F. Malandrino, C. Casetti, C.-F. Chiasserini, Z. Limani, Fast resource scheduling in HetNets with D2D support, in: INFOCOM, 2014 Proceedings IEEE, IEEE, 2014, pp. 1536–1544.
- 1059
- 1060 [51] Q. Wang, M. Hempstead, W. Yang, A realistic power consumption model for wireless sensor network devices, in: Sensor and Ad Hoc Communications and Networks, 2006. SECON'06, 1, IEEE, 2006, pp. 286–295.
- 1061
- 1062 [52] N. Karmarkar, A new polynomial-time algorithm for linear programming, in: 2006 Third Annual IEEE Communications Society on Proceedings of the Sixteenth Annual ACM Symposium on Theory of Computing, ACM, 1984, pp. 302–311.
- 1063
- 1064
- 1065
- 1066
- 1067
- 1068
- 1069
- 1070
- 1071